CIVIL ENGINEERING DEPARTMENT

DYNAMIC VIBRATION TECHNIQUES IN HIGHWAY BRIDGE MONITORING

John T DeWolf, Professor
Jun Zhao, Graduate Research Assistant

Final Report
May, 1998

Report CEE-98-1

SCHOOL OF ENGINEERING
UNIVERSITY OF CONNECTICUT
STORRS, CONNECTICUT

DYNAMIC VIBRATION TECHNIQUES IN HIGHWAY BRIDGE MONITORING

John T DeWolf, Professor
Jun Zhao, Graduate Research Assistant

Final Report
May, 1998

Report CEE-98-1

This research was sponsored the Connecticut Department of Transportation and was carried out in the Civil and Environmental Department of the University of Connecticut.

Technical Report Documentation Page

1. Report No.	2.	3. Recipient's Catalog No.
CEE -98-1	PB99-140857	

4. Title and Subtitle	5. Report Date
Dynamic Vibration Techniques in Highway Bridge Monitoring	May, 1998
	6. Performing Organization Code

7. Author(s)	8. Performing Organization Report No.
John T. DeWolf and Jun Zhao	

9. Performing Organization Name and Address	10 Work Unit No. (TRAIS)
University of Connecticut Department of Civil and Environmental Engineering 191 Auditorium Road, Box U-37 Storrs, CT 06269	11. Contract or Grant No. CT-SPR-Study Number 2217
12. Sponsoring Agency Name and Address	13. Type of Report and Period Covered
Connecticut Department of Transportation 280 West Street Rocky Hill, CT 06067-0207	Final Report 14. Sponsoring Agency Code SPR-2217

15 Supplementary Notes

A study conducted in coperation with the US Department of Transportation, Federal Highway Administration.

16. Abstract

Currently, there are different monitoring techniques which can be used for damage detection in bridges. These include approaches based on both static and dynamic behavior. The use of dynamic properties has advantages over static properties, since components of the dynamic properties are only marginally influenced by variations in the loading. When dynamic properties are used, field studies have shown that it is not always sufficient to use only the traditional natural frequencies and modal displacements. Current research on bridge damage detection indicates that derivatives of natural frequencies and modal displacements, including the modal flexibility, the modal assurance criterion, and the coordinate model assurance criterion, may be used to generate effective diagnostic parameters for damage identification. This report presents a review of all current methods which use vibrational information for bridge monitoring and damage detection. The methods are applied to the results from a field study of a bridge in which expansion bearings were partially restrained in colder weather.

17. Key Words	18. Distribution Statement
Bridge Monitoring, Connection Behavior, Dynamic Behavior, Steel Bridges, Testing, Vibrational Monitoring	

19. Security Classif. (of this report)	20. Security Classif. (of this page)	21. No. of Pages	22. Price
unclassified	unclassified	45	

Form DOT F 1700.7 (8-72) Reproduction of completed page authorized

SI* (MODERN METRIC) CONVERSION FACTORS

APPROXIMATE CONVERSIONS TO SI UNITS

Symbol	When You Know	Multiply By	To Find	Symbol
		LENGTH		
in	inches	25.4	millimetres	mm
ft	feet	0.305	metres	m
yd	yards	0.914	metres	m
mi	miles	1.61	kilometres	km
		AREA		
in^2	square inches	645.2	millimetres squared	mm^2
ft^2	square feet	0.093	metres squared	m^2
yd^2	square yards	0.836	metres squared	m^2
ac	acres	0.405	hectares	ha
mi^2	square miles	2.59	kilometres squared	km^2
		VOLUME		
fl oz	fluid ounces	29.57	mililitres	mL
gal	gallons	3.785	Litres	L
ft^3	cubic feet	0.028	metres cubed	m^3
yd^3	cubic yards	0.765	metres cubed	m^3

NOTE: Volumes greater than 1000 L shall be shown in m^3

		MASS		
oz	ounces	28.35	grams	g
lb	pounds	0.454	kilograms	kg
T	short tons (2000 lb)	0.907	megagrams	Mg
		TEMPERATURE (exact)		
^0F	Fahrenheit temperature	5(F-32)/9	Celcius temperature	^0C

* SI is the symbol for the International System of Measurement

APPROXIMATE CONVERSIONS TO SI UNITS

Symbol	When You Know	Multiply By	To Find	Symbol
		LENGTH		
mm	millimetres	0.039	inches	in
m	metres	3.28	feet	ft
m	metres	1.09	yards	yd
km	kilometres	0.621	miles	mi
		AREA		
mm^2	millimetres squared	0.0016	square inches	in^2
m^2	metres squared	10.764	square feet	ft^2
ha	hectares	2.47	acres	ac
km^2	kilometres squared	0.386	square miles	mi^2
		VOLUME		
mL	millilitres	0.034	fluid ounces	fl oz
L	litres	0.264	gallons	gal
m^3	metres cubed	35.315	cubic feet	ft^3
m^3	metres cubed	1.308	cubic yards	yd^3
		MASS		
g	grams	0.035	ounces	oz
kg	kilograms	2.205	pounds	lb
Mg	megagrams	1.102	short tons (2000 lb)	T
		TEMPERATURE (exact)		
^0C	Celcius temperature	1.8C+32	Fahrenheit temperature	^0F

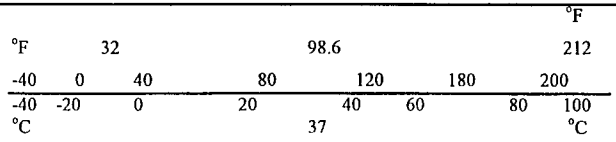

TABLE OF CONTENTS

TABLE OF CONTENTS (CONTINUED)

LIST OF FIGURES

LIST OF FIGURES (CONTINUED)

LIST OF FIGURES (CONTINUED)

INTRODUCTION

The Federal Highway Administration has estimated that nearly one-third of the bridges in the country need to repaired or replaced. Approximately 11 percent are structurally deficient. Most bridges are presently monitored with visual inspections, normally at two year intervals. This approach obviously does not address changes which may occur between inspections. Additionally, it does not use rapidly expanding technology for assessment.

Currently, there are different monitoring techniques used for bridge monitoring and damage detection, including those based on static behavior and some based on dynamic behavior. During the past decade, many research studies have focused on the possibility of using the vibrational characteristics of structures as an indication of structural condition. The use of dynamic properties has advantages over use of static properties, since components of the dynamic properties are only marginally influenced by variations in the loading which occur with different vehicles, vehicle speeds and lane positions.

Since bridges are complex structures, the dynamic behavior is represented by a number of coupled modes. These contribute to the measured response. Since the local modes for the bridges fall into the same range as the global modes, field studies have shown that it is not always sufficient to use only the traditional frequencies and mode shapes. Current research on bridge damage detection indicates that derivatives of natural frequencies and mode shapes, such as modal flexibility, modal assurance criterion, and coordinate modal assurance criterion, may be used to generate effective diagnostic parameters for damage identification.

This report presents a review of different methods based on vibrational information which may be used for bridge monitoring and damage detection. The methods are used to evaluate a bridge in which the bearings were partially restrained in colder weather, as demonstrated by the field test data. The bridge was monitored using a vibrational monitoring system developed by Vibra-Metrics of Hamden, Connecticut.

LITERATURE REVIEW

The following is a review of studies which use dynamic behavior as a basis of monitoring the structural integrity of bridges.

Based on a laboratory study with a bridge model, a two span aluminum plate-girder bridge subject to moving loads, Mazurek and DeWolf (1990) concluded that the ambient vibrational approach, based on a moving vehicle, could provide a feasible bridge monitoring technique. The study indicated that major deterioration was detectable by

comparisons of natural frequencies and mode shapes. The conclusion was verified using a finite element analysis.

Gaghavendrachar and Aktan (1992) studied the analytical and experimental application of modal flexibility for structural monitoring of an actual three-span concrete bridge. A multi-reference impact testing method, based on an applied known hammer load, was used in the study. Modal flexibility uses both natural frequencies and mode shapes as defined in the next section of this report. Modal flexibility is reported to be sensitive to local damage and can be a reliable indicator for structural damage identification. A finite element model was used to assist in the interpretation of the results and was improved and calibrated based on field measurements. Truck-load tests were conducted to verify the reliability of the calibrated finite element model. The study demonstrated that modal flexibility is influenced by local modes and more sensitive to localized conditions than changes in frequency or mode shapes. The study concluded that modal flexibility may be regarded as a reliable index for damage detection if the variations in flexibility coefficients are interpreted with sound engineering judgment and expertise.

Chang, Shen and Lee (1993) used a wide-flange steel beam with four types of artificially introduced cracks in the web and flanges to study damage detection. Nine accelerometers and nine strain gages were used. Using the impact technique, frequencies, displacement mode shapes (DMS) and strain mode shapes (SMS) were obtained from frequency response functions. Comparisons were made to determine if these parameters were useful in detecting cracks. This study concluded that web cracks had an insignificant affect on the dynamic parameters. Experimental evaluation of frequency was more reliable when compared to the use of the damping ratios. SMS was most sensitive in detecting the damage zone, as compared to other modal parameters.

Lauzon (1995) monitored a full-scale three-span highway bridge with rolled steel beams and a concrete deck. The bridge was in the process of being demolished and replaced, after over 40 years of service. The flange and web of one of the exterior of three girders was incrementally cut to approximate a crack. It was expected that this girder would be most likely to develop a crack. The bridge was excited with a test vehicle and vibrational data was obtained using eight accelerometers attached to the steel girders. The data was then transformed to frequency spectra. The study concluded that changes were detectable from the vibrational information, especially for a more significant cut. It is also noted that a change in the frequency with the highest acceleration could be used in determining structural changes.

Based on monitoring of a continuous two span bridge, DeWolf, Conn and O'Leary (1995) studied the changes in the dynamic behavior in a bridge in which the end bearings were partially restrained at lower temperatures. The bridge was excited by routine traffic and monitored remotely with a fully operational remote vibrational monitoring system with 16 accelerometers. The monitoring system was used to collect

accelerations and process the data to develop the mode information. The bridge's performance was evaluated during both summer and winter. The study indicated that lower temperatures resulted in partially restrained bearings, which in turn introduced axial tensile forces into the girders. This led to increased natural frequencies. Fu (1996) and DeWolf and Fu (1997) used finite element analysis models to study the influence of temperature and cracking on the frequencies and mode shapes in this bridge. The study concluded that the changes in temperature resulted in changes in some frequencies. The conclusion that changes in the frequency response were due to partial restraint of the end bearings as a result of a drop in temperature was verified.

Law, Ward, Shi, Chen, Waldron and Taylor (1995) determined the capacities of an one-fifth scale model bridge with a reinforced-concrete deck and steel girders. This bridge deck was tested to destruction. The vibrational response to ambient excitation was measured at different stages of cracking and spalling in the concrete deck. The study considered the changes in natural frequencies, strains, displacements, neutral axis depth, cracking moments, and the effect on the steel beam due to cracking and spalling of the concrete deck. The results demonstrated that the loading capacity of a beam could be expressed as a function of the percentage of reinforcement in the member and the cracked moment of inertia. The fundamental frequency of the structure was not sensitive to local damage in the bridge deck.

Shelley (1995) studied an one-span steel truss bridge which was scheduled for demolition. Damage was introduced in two chords. The bridge was excited by an actuator. Differences in modal flexibility before and after damage were identified. Prior to the demolition of the bridge, Shelley, Lee, Aksel and Aktan (1995) conducted nondestructive tests on the bridge instrumented with 26 accelerometers in both vertical and horizontal directions. The changes in the resonant frequencies were determined with the system, and they were used to indicate damage. The approach was successful in identifying damage 90% of the time.

Toksoy and Aktan (1995) tested an existing three-span reinforced concrete slab bridge. They used a small impact hammer to excite the bridge. The modal flexibility was obtained by processing data from 11 accelerometers from impact modal testing. A finite element analysis model of the bridge, which was calibrated with data from the bridge, was selected to produce a baseline for modal flexibility comparison. The study indicated that the maximum frequency shift between undamaged and damage condition was questionable because of experimental and post-processing errors, and because of the influence of the ambient noise. In contrast with frequencies and mode shapes, significant differences in modal flexibility occurred. There was a maximum 5% difference in frequency, which produced a 40% difference in modal flexibility.

Aktan, Lee and Dalal (1995) experimentally determined the modal flexibility in seven highway bridges using impact testing to develop a structural condition index.

Included were two continuous, three-span reinforced concrete skewed slab bridges, three three-span steel-stringer bridges, and two steel through-truss bridges. Finite element analysis models were calibrated with experimental data and used to produce baseline information. One of the bridges was loaded by simulating progressively increasing stationary truck loading with hydraulic actuators. A significant discrepancy in modal flexibility before and after the loading was observed in the vicinity of the loading area. They suggested that 20 mode shapes should be sufficient to obtain an accurate measure of a bridge's flexibility. Due to linearization and unavoidable experimental errors inherent in modal testing of large constructed facilities, they concluded that the maximum reliability of detecting presence of damage using the modal flexibility of a bridge should not be expected to exceed 90% (9 out of 10 bridges with damage would be detected). They also concluded this type of reliability would be adequate to evaluate damage of a structure if the modal flexibility method is combined with other techniques such as visual evaluation, proof-load tests, and measurements of the current state of a structure in terms of available strength, deformation and energy dissipation capacities.

Stubbs and Sikorsky (1995) used pattern recognition techniques to classify the response of structures into defined categories. Damage information was obtained through visible plots of the "damage location indicator" which is based on mode shapes and material properties of structures. They tested one span of an actual three-span plate-girder bridge to verify the technique using modal testing techniques. Damage included four cracks in the flanges and webs of girders. Eleven accelerometers were used, producing three mode shapes. The location of the cracks was detected using the indicator.

Kim and Stubbs (1995) studied the impact of mode uncertainty on damage detection for the cases which only a few mode shapes were available. They used the same damage indicator as used in the study by Stubbs and Sikorsky (1995) for the laboratory results from a two-span aluminum model girder test conducted by Mazurek and DeWolf (1990). The damage detection accuracy for the model girder, in which there were a number mode shapes available, was estimated as a function of model uncertainties. This study presented an approach to predict damage location and severity when there is only limited mode information. The study included evaluation of the damage in an environment of uncertainty due to modeling errors and modal response measurement errors.

Alampalli, Fu and Dillon (1995) tested an abandoned bridge with five steel girders and a 1/6 scale model based on this bridge. They studied the sensitivity of modal parameters for determining damage. Damage was introduced by cuts in both structures, and the impact test method was used. The structural signatures used in the tests were modal frequencies, mode damping ratios, mode shapes, modal assurance criterion (MAC) and coordinate modal assurance criterion (COMAC). Environmental influences, including temperature fluctuations and mechanical vibrational noise, were also considered. The testing results demonstrated that the damping ratio is not a stable modal parameter.

Frequencies, mode shapes, MAC and COMAC values can be estimated with relatively higher consistency in damage detection. The study concluded that modal frequencies may be used to detect the existence of damage or deterioration in highway bridges, and cross-diagnosis using multiple signatures such as mode shapes, MAC and COMAC are warranted for such detection because a single signature may not be conclusive due to inevitable variations in the measured data. The study indicated that a limited number of modes may be inadequate for damage diagnosis with high confidence, because certain modes may be less sensitive to the damage or may include higher noise leading to false diagnosis.

Chen and Kim (1995) studied damage detection in a model of a steel truss-type bridge structure instrumented with five accelerometers and five strain gauges. The model had two tube girders. The damage was simulated with sawcuts in one flange and both webs of tubes. Their analysis was based on a neural network, which considered comparisons between accelerations and strains. Vibrational signals were measured from a series of experiments with the impact testing technique. The results of the study showed that neural networks provide a promising approach as a computing tool required for autonomous signal monitoring of instrumented structures. The recognition of damage severity was less accurate than that of damage location. Sensor signals, accelerometers and strain gauges, used as inputs to the network, were feasible for damage identification.

Lauzon (1997) expanded the analysis of his 1995 study (Lauzon, 1995; Lauzon and DeWolf, 1993, 1995) involving a destructive test of a full-scale bridge in which a crack was introduced into the external girder. In addition to the natural frequencies and mode shapes, he used the signature assurance criterion (SAC) and cross signature assurance criterion (CSAC) to analyze the data in the test. These methods are similar to the MAC and COMAC. The difference is that the SAC and CSAC use acceleration data directly, instead of using mode shapes which are processed from the acceleration as done with the MAC and COMAC. The results from CSAC provided better indications of the changes in the stiffness than provided by SAC. Two finite element analysis models, based on one dimensional and two dimensional models, were also used to predict the changes in the frequencies caused by the cracks.

SUMMARY OF LITERATURE REVIEW

Diagnostic Parameters

The most common diagnostic parameters currently used in bridge monitoring and damage detection are Natural Frequencies and Mode Shapes (Stubbs, Kim and Topole in 1992; Lauzon and DeWolf in 1993; DeWolf, Conn and O'Leary in 1995; Law, Ward, Shi, Chen, Waldron and Taylor in 1995; Kim and Stubbs in 1995; Lauzon in 1995; Alamalli, Fu

and Dillon in 1995; Lauzon and DeWolf in 1996); the derivatives of natural frequencies and mode shapes such as Modal Assurance Criterion (MAC), Signature Assurance Criterion (SAC), Cross Signature Assurance Criterion (CSAC), and Coordinate Modal assurance Criterion (COMAC) (Alapalli, Fu and Dillon in 1995; Lauzon in 1997); Modal flexibility (Gaghavendrachar and Aktan in 1992; Shelley in 1995; Toksoy and Aktan in 1995; Aktan, Lee and Dalal in 1995); and Strain Mode Shapes (SMS) (Chang, Shen and Lee in 1993).

Load Excitation

There are two general approaches to exciting a bridge, either with some form of impact hammer (impact loading) or with the ambient approach (traffic). In the former, the loading is fully defined, and thus can be used with the response to define the vibrational parameters. In the latter, the loading is not fully defined. Thus it is necessary to consider variations in the vibrational parameters which occur because of the variations in loading amplitude and location.

Often, the impact testing technique is a useful tool in structural engineering for vibrational monitoring. The major use of the impact technique is to estimate modal parameters and mode shapes from the frequency response functions. Some researchers have used this technique for bridge damage detection (Raghavendrachar and Aktan in 1992; Aktan, Lee and Dalal in 1994; Toksoy and Aktan in 1993; Alampalli, and Fu in 1994; Alampalli, Fu and Dillion in 1995). Halyorsen and Brown (1995) reviewed the procedures for using the impact technique as related to modal analysis, along with problems encountered in its use. They discussed nonlinearity in structures and the equipment required for impact testing. The main advantage for impact testing is that energy in an impact is distributed continuously in the frequency domain, rather than occurring at discrete spectral lines, as in the case of periodic signals from sinusoidal sweeping forces. Thus, an impact force can excite a large number of natural frequencies. In a large bridge, it is necessary to provide sufficient energy to excite these modes. Hydraulic actuators are thus often used in testing. They provide static and sinusoidal sweeping loading, and they can easily control the amplitude and frequency of loading. This type of exciting facility was used by Shelley (1995), Aktan, Lee and Dalal (1995).

An alternative to impact loading is the ambient approach. This is based on normal traffic loading, and it is convenient and economical for routine bridge monitoring. Bridges can be easily and remotely monitored using the ambient approach. Variations in frequency response due to variation in the vehicle types and lane locations must be incorporated in the analysis. Lauzon and DeWolf (1993), DeWolf, Conn and O'Leary (1995), and Lauzon (1995 and 1997) have used this type of loading in bridge monitoring. Tables 1 and 2 summarize the diagnostic parameters and load excitation used for bridge monitoring and damage detection.

The literature review has shown that:

1. Some natural frequencies and mode shapes are not sensitive to specific types of damage. In general, use of individual natural frequencies and mode shapes are not as useful for damage detection as techniques which are based on a combination of frequencies and mode shapes.

2. Damping coefficients are not reliable parameters in bridge damage detection because of the uncertainties in determining the damping values.

3. Damage in bridges may be quantitatively recognized with mode shapes, frequency spectra, the modal assurance criterion, the signature assurance criterion, the coordinate modal assurance criterion, the cross signature assurance criterion and the modal flexibility.

4. Types of loads that have been used in monitoring are normal traffic, an impact hammer, and hydraulic actuators.

5. The use of multiple diagnostic parameters should provide more reliable results than any technique using a single parameter.

Table 1. Diagnostic Parameters Used in Bridge Monitoring and Damage Detection

Diagnostic Parameters	Description of Parameters	Bridge Tested	Researchers Who Used Parameters
Natural Frequencies	Basic parameters in bridge monitoring.	One-span bridge with three steel girders; continuous two-span bridge with a concrete slab and seven steel girders; one-span bridge with five steel girders.	1). Stubbs, Kim & Topole; 2). Lauzon & DeWolf; 3). DeWolf, Conn & O'Leary; 4). Law, Ward, Shi, Chen, Waldron & Taylor; 5). Alamalli, Fu & Dillon.
Mode Shapes 1. Displacement Mode Shapes; 2. Acceleration Mode Shapes; 3. Strain Mode Shapes.	Basic parameters in bridge monitoring.	One-span bridge with three steel girders; three-span bridge with rolled beams; continuous two-span bridge with a concrete slab and seven steel girders; one-span bridge with five steel girders.	1). Stubbs, Kim & Topole; 2). Lauzon & DeWolf; 3). DeWolf, Conn & O'Leary; 4). Law, Ward, Shi, Chen, Waldron & Taylor; 5). Alamalli, Fu & Dillon; 6). Chang, Shen & Lee; 7). Chang, K.C, Shen, Z. and Lee, G.C.
Damping Ratio	Not commonly used; unreliable parameters due to the difficulty of determining damping values.	One-span bridge with five steel girders.	Alampalli, Fu & Dillon.
Modal flexibility	Derivatives of natural frequencies and mode shapes. Used in damage detection for bridges, sensitive to local damage.	Three-span concrete bridge; steel truss bridge; Two continuous three-span reinforced concrete slab bridges; Two steel truss bridges; Three three-span steel stringer bridges.	1). Gaghavendrachar & Aktan; 2). Shelley & et al.; 3). Toksoy & Aktan; 4). Aktan, Lee & Dalal.
Modal assurance Criterion (MAC)	Derivatives of mode shapes. Comparisons between two mode shapes.	Simple bridge with five steel girders.	1). Alampalli, Fu & Dillon; 2). Lauzon.
Coordinate Modal assurance Criterion (COMAC)	Derivatives of mode shapes. Comparisons between two sets of mode shapes.	Simple bridge with five steel girders.	1). Alampalli, Fu & Dillon; 2). Lauzon.
Artificial Neural Networks	Training data from either field or computer simulation. Approximation of testing data is based on trained networks.	A model of a steel truss-type bridge structure.	1). Chen, S. S. and Kim, Sungkon.

Table 2. Loading Used in Bridge Monitoring and Damage Detection

Loading Excitation	Brief Description of Loading	Bridge Tested	Researchers Who Used Loading
Normal Traffic Vehicle	The amplitude and location of loading on bridges varies.	One-span bridge with three steel girders; continuous two-span bridge with a concrete slab and seven steel girders' continuous reinforced concrete arched bridge.	1). Lauzon & DeWolf; 2). DeWolf, Conn & O'Leary; 3). Sartor & DeWolf.
Impact Loading	Provides wide range of input frequency and can be used to obtain frequency response functions combined with adequate vibrational equipment. Not always able to provide sufficient energy to excite large bridges.	Three-span concrete bridge; two continuous three-span reinforced concrete slab bridges; two steel truss bridges; three three-span steel stringer bridges; three-span reinforced concrete slab bridge; simple bridge with five steel girders.	1). Raghavendrachar & Aktan; 2). Aktan, Lee & Dalal; 3). Toksoy & Aktan; 4). Alampalli & Fu; 5). Alampalli, Fu & Dillion.
Hydraulic Actuators	Similar to Impact Loading. Provides sufficient energy, compared to impact loading.	One-span steel truss bridge; two continuous three-span reinforced concrete slab bridges; two steel truss bridges; three three-span steel stringer bridges.	1). Shelley & et al.; 2). Aktan, Lee & Dalal.

TECHNIQUES FOR MONITORING

This section contains a review of the different vibrational parameters used for monitoring, including techniques for processing these parameters.

Damage Detection

The basic modal parameters for monitoring bridges are the natural frequencies and mode shapes. In addition to these traditional parameters, additional diagnostic parameters may be derived from the mode shapes and frequencies. The modal flexibility, modal assurance criterion and coordinate modal assurance criterion are obtained from the frequencies and/or mode shapes.

The following describes how each of the parameters is determined.

1. Natural Frequencies

Natural frequencies may be determined experimentally, or determined analytically from methods such as a finite element analysis.

2. Mode Shapes

Mode shapes associated with the specific natural frequencies can be based on acceleration, displacements, or strains.

(1) Acceleration mode shapes: these may be obtained experimentally from frequency spectra by processing accelerations using Fast Fourier Transform (FFT).

(2) Displacement mode shapes: displacement mode shapes may be determined directly from displacement sensors, or approximated from acceleration data.

(3) Strain mode shapes: strain mode shapes may be determined from readings of strain gages.

3. Modal Flexibility

The modal flexibility includes the influence of both the mode shapes and the frequencies. It is defined as the accumulation of the contributions from all available modal vectors and corresponding natural frequencies. In practice, the mode shapes should be unit mass mode shapes (unit mass orthogonal mode shapes). Using this parameter, the changes in dynamic properties of bridges can be found in both plots and quantitative analysis.

The modal flexibility matrix $[F]_{n*m}$ is defined (Hoyos and Aktan, 1987) as

$$[F]_{n\bullet m} = [\phi]^T_{n\bullet m}[\frac{1}{\omega^2}][\phi]_{n\bullet m} \quad (1)$$

where $[F]_{n\bullet m}$= modal flexibility matrix of a structure;
$[\phi]$ = unit-mass scaled mode matrix which satisfies $[\phi]^T[M][\phi] = [I]$ ([I] is an unit matrix).
n = number of measurement points;
m = number of modes; and
$[\frac{1}{\omega^2}]$ = diagonal matrix of ascending natural frequencies.

The modal flexibility matrix determined from Equation (1) is symmetric and has dimensions equal to the number of natural frequencies and mode shapes which are obtained from the monitoring.

4. Modal Assurance Criterion (MAC)

The MAC indicates the degree of correlation between two measured mode shapes at a specific natural frequency from two different tests. The values in the MAC, which is a two dimensional array, vary from 0.0 to 1.0, with 0.0 for no correlation and 1.0 for full correlation. The MAC calculated from two identical mode shapes will result in a unit value. The MAC is defined as

$$\text{MAC(j, k)} = \frac{(\phi^T_{Aj}\phi_{Bk})^2}{(\phi^T_{Aj}\phi_{Aj})(\phi^T_{Bk}\phi_{Bk})} \quad (2)$$

where $j = 1,2,...m_A$ and $k = 1,2,..m_B$;
m_A and m_B = the dimension of each of the mode shapes for $[\phi_A]$ and $[\phi_B]$, respectively;
ϕ_{Aj} = the ith coordinate of the jth column (mode) of $[\phi_A]$;
ϕ_{Bk} = the ith coordinate of the kth column (mode) of $[\phi_B]$; and
$[\phi_A]$ and $[\phi_B]$ are two sets of mode shapes and can be corresponding to original and testing mode shapes.

The size of the MAC depends on the number of mode shapes used. If some elements have been damaged, the resulting mode shapes will be different from the original ones, and the MAC determined from the undamaged and damaged mode shapes will be between 0.0 and 1.0. Thus, the MAC can be useful to detect the existence of damage and provide global damage information. It is noted that each value of the MAC uses two mode shapes, as opposed to the COMAC which follows.

The signature assurance criterion (SAC) which is similar to the MAC was used by Lauzon (1997) for an actual bridge monitoring. The difference between the SAC and the MAC is that the SAC uses accelerations directly from the sensors, while the MAC uses deflected mode shapes which can be approximated by nondimensionalized accelerations.

5. Coordinate Modal Assurance Criterion (COMAC)

The COMAC represents the correlation between two measured mode shapes at a specific natural frequency from two different tests. Unlike the MAC, the COMAC considers the values all mode shapes at a specific point on the structure. The COMAC identifies where the mode shapes agree or do not agree, indicating potential damage. The COMAC is defined as

$$COMAC(i) = \frac{(\sum_{l=1}^{n} \phi_{Al,i}\phi_{Bl,i})^2}{(\sum_{l=1}^{n} \phi_{Al,i}^2)(\sum_{l=1}^{n} \phi_{Bl,i}^2)} \qquad (3)$$

where $\phi_{Al,i}$ is the ith term of lth mode shape in the A set of mode shapes;
$\phi_{Bl,i}$ is the ith term of lth mode shape in the B set of mode shapes; and
n is the number of the mode shapes.

The size of the COMAC depends on the number of mode shapes used. If $[\phi_A]$ and $[\phi_B]$ are identical, the COMAC will be equal to unity, indicating there is no difference between the two sets of test data.

Both the MAC and the COMAC use mode shape information only, unlike the modal flexibility which uses both frequencies and mode shapes.

The cross signature assurance criterion (CSAC) as used by Lauzon (1997) for an actual bridge monitoring is similar to the COMAC. The difference between CSAC and COMAC is that is the same as the difference between the MAC and SAC. Thus, the CSAC uses the accelerations directly from the sensors, and the COMAC uses mode shapes determined from the accelerations.

Damage Location and Severity

The previous material presents different techniques for determining whether damage exists. Two other interests are determining the location where the damage occurs and the severity of the damage, i.e. how likely it is to cause structural failure. Determination of the severity is especially difficult because there are variations in different bridge structures, and many factors influence the likelihood of structural failure.

Stubbs, Kim and Topole (1992) presented an approach using a Damage Indicator and a Damage Location Indicator. These are based on mode shapes and material properties. The method can not always be used in practice because the required structural information, material properties and stiffness, is not always available. Nevertheless this method is described here because it is the only published study related to damage severity for bridges.

6. Damage Location Indicator

The damage location indicator, β_j , produces damage severity information. Damage at *j*th member is indicated if $\beta_j > 1.0$ (Stubbs et al. 1992). From this, the location of damage at *j*th member can be identified if β_j is larger than a unit value. The advantages of the indicator are that only mode shapes and material properties are needed. Often, damage can be located using a few mode shapes. This requires solution of a single equation. The disadvantage is that a number of mode shapes and material properties must be determined in advance. The value of β_j is given as

$$\beta_j = \frac{\sum_{i=1}^{NM} \phi_i^{*T} C_{jo} \phi_i^* K_i}{\sum_{i=1}^{NM} \phi_i^T C_{jo} \phi_i K_i^*} \qquad (4)$$

where ϕ_i^* and ϕ_i are the ith damaged and undamaged mode shapes;

$K_{ij} = \phi_j^T C_j \phi_i$, where K_{ij} is the contribution of the jth member to ith mode stiffness;

$C_j = E_j C_{jo}$, is the contribution of jth member to the system stiffness matrix;

E_j is modulus of elasticity of ith member; and

C_{jo} involves geometric quantities and the terms containing Poisson's ratio and can represent bending, torsion, axial, shear, or even plate elements.

7. Damage Severity Indicator

This indicates the severity of damage. No damage exists if $\alpha_j = 0.0$ (β_j=1.0), otherwise damage exists. This indicator is defined as

$$\alpha_j = \frac{1}{\beta_j} - 1, \text{ and } -1.0 \le \alpha_j \le 0.0 \qquad (5)$$

A case of extreme damage would have a value of α_j = - 1.0. More severe damage would be indicated with smaller values of α_j.

8. Artificial Neural Networks

Artificial Neural Networks (ANN) are computational models composed of many simple and highly interconnected processing elements which process information and establish complex relationships and associations from large sets of data. They stand in contrast with traditional techniques which establish relationships with known mathematical algorithms. By the approaches of ANN, the data required to model an inverse relation are obtained as the solution of the direct problem. For example, the changes in some structural parameters can be identified from the known structural response when the network has been trained properly. Neural networks are capable of modeling input-output functional relations after training. Thus the acceleration data, or other data collected from sensors, is fed directly to the ANN without processing. An application of ANN to bridge monitoring has been carried out by Chen and Kim (1995). They were able to identify the damage location and severity based on tests of a bridge model.

FIELD STUDY OF A BRIDGE

In this report, the approaches as previously presented for evaluating vibrational behavior are used to evaluate changes in the bridge reported by Conn in 1994, DeWolf, Conn and O'Leary in 1995, and by Conn and DeWolf in 1995. The goal of the study is to identify the changes in the structural behavior at different temperatures, due to partial restraint in the expansion bearings of the bridge.

Bridge Description

The bridge used in this study was built in 1954. It has two equal length spans, and is continuous at the center support. It has a concrete slab which was not designed to behave compositely with seven non-prismatic welded steel plate girders. Nevertheless, it behaves compositely under normal vehicle loading. The cross-section is shown in Figure 1.

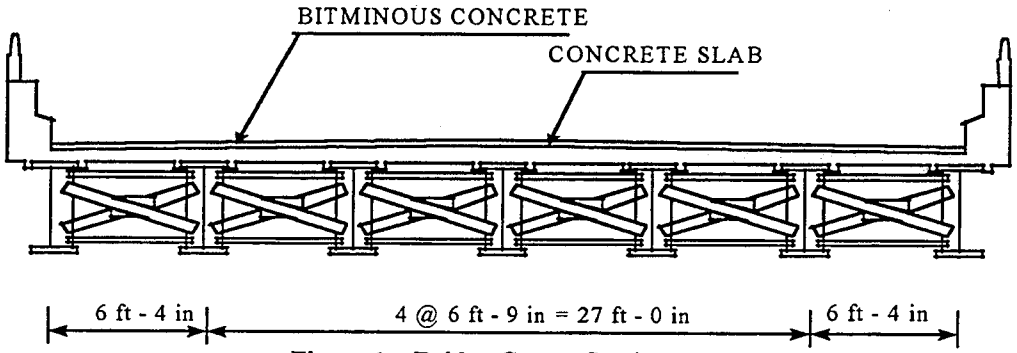

Figure 1 Bridge Cross - Section

Test Data

A permanent monitoring system was used to collect accelerations and process the data to develop the modal information. The accelerations of the bridge were obtained with 16 accelerometers mounted to the bridge. The resulting measurements were analyzed using Fast Fourier Transformation (FFT) into frequency spectra. The accelerometer locations are shown in Figure 2. Fourteen channels functioned properly. Accelerometers 5 and 11 gave erroneous results during the testing period.

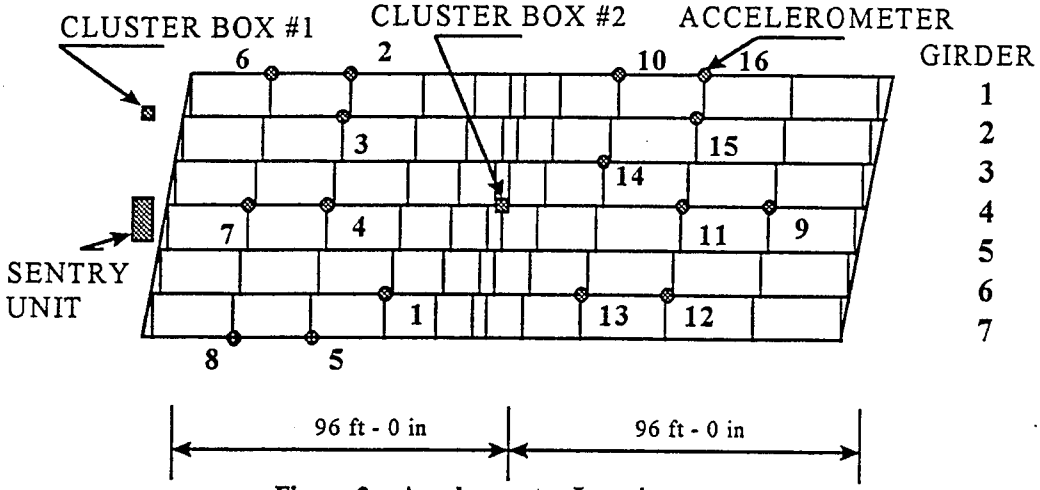

Figure 2 Accelerometer Locations

A typical frequency spectrum, taken during one collection period, is shown in Figure 3. This plots the volts (proportional to acceleration) versus frequency. The natural frequencies are associated with peaks in this diagram. However, not all peaks correspond to natural frequencies, and it is thus necessary to verify the natural frequencies using a modal analysis.

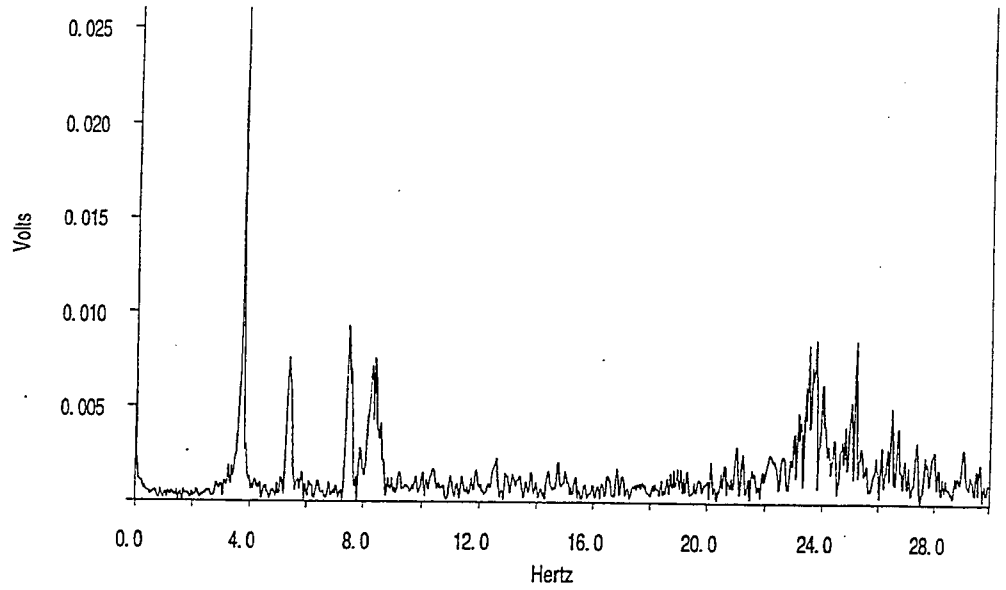

Figure 3 Typical Frequency Spectrum

The bridge's mode shapes were obtained from the frequency spectra by normalizing the accelerations associated with each natural frequency. The phase angles for each accelerometer were used to verify the mode shapes. Two mode shapes, the first bending mode shape, and the first torsion mode shape, are shown in Figures 4 and 5. The second bending mode shape was also established from the test results.

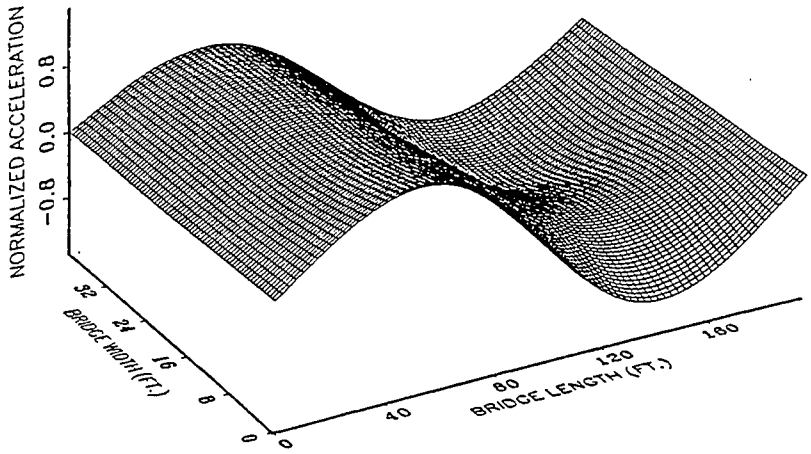

Figure 4 First Bending Mode Shape

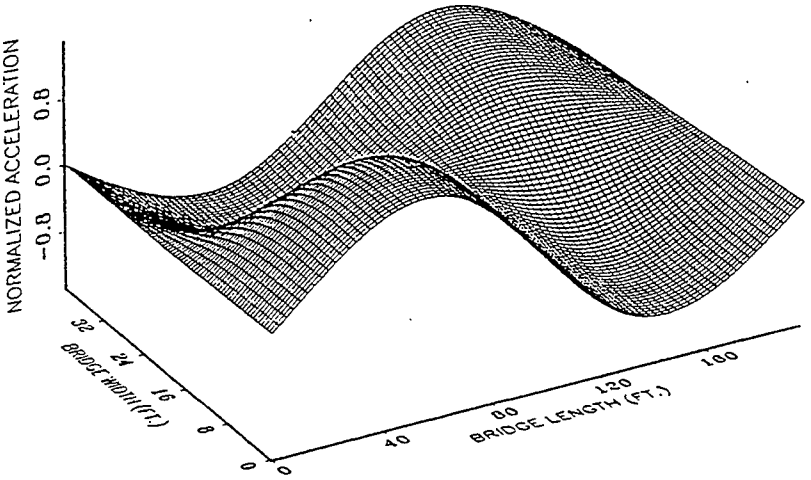

Figure 5 First Torsional Mode Shape

Each set of data collected in the field included the raw accelerations for the 14 channels and the ambient air temperatures. The bridge was evaluated and found to be in sound condition. However, changes in the vibrational data occurred when the temperature changed (Conn, 1994). It was concluded that these changes were due to partially restrained bearings. Decreases in temperature produced additional axial tensile forces in the girders of the bridge. This resulted in increases in the stiffness and the frequencies.

Table A1 in the Appendix contains data for the 16 sets of the normalized accelerations for the fourteen properly functioning channels. Each set of data was obtained from processing field data using the Fast Fourier Transform, with determination of the phase angles to verify the modal displacements. Each set corresponds to the previously determined resonant frequencies determined in the previous studies (Conn, 1994). Thus there are three modal displacements in each data set. Each of the modal displacements was normalized based on the maximum acceleration value in the mode shape. The three modal displacements are defined as first and second bending modal displacements, and the first torsional mode shape. Totally, there are 16 sets of data available.

There were 4 sets of bad data (at the temperatures of 18F°, 19F° and 40F°). The data for these sets were bad because the data for the accelerometers 4, 6, 8 and 9 (refer to the shaded sets in Table A1 in the Appendix) were not reasonable for first torsional modal displacements. The nonzero value for accelerometer 7 in data set 8, and the zero values for the accelerometers 2, 6, 8, 14 and 16 in data sets 14, 15 and 16 do not produce a clear first torsional mode shape. The cause of this is probably due to lack of sufficient excitement in these data runs. In order to evaluate the effectiveness of each technique, the four sets of bad data will be included in the analysis.

APPLICATION OF EVALUATION TECHNIQUES

The natural frequencies, the modal displacements, the modal flexibility, the MAC and the COMAC are separately used to evaluate the bridge in this report. As noted previously the MAC and COMAC are essentially the same as the SAC and CSAC. The goal is to determine the feasibility for using these approaches in bridge monitoring.

Conn (1994) has shown that when the temperature was less than approximately 60°F, the three lowest natural frequencies increased. Thus the two sets of data with the same temperature of 55°F are used herein as baseline 1 and baseline 2. All sets of data, given in the Appendix, for lower temperatures are compared with the baselines to determine the feasibility of using each of the analytical approaches to predict the changes in the structural behavior due to the partial restraint in the bridge's end bearings.

Natural Frequencies

All sets of data for the frequencies as listed in Table A1 are used to demonstrate how variations in temperature influence the variations in the natural frequencies. The baseline frequencies were those obtained at 55°F. Figure 6 shows the changes in natural frequencies with temperature. The change is shown as the percentage change from the appropriate frequencies at 55°F. Four sets of data collected at the temperatures of 18°F, 19°F, and 40°F did not contain sufficient excitement to fully define the modal properties. These sets of data are referred as bad data. It is clear that the frequencies for the bad sets are not fully consistent with the changes at the other temperatures. The maximum changes in the natural frequencies were 11.6% for the first frequency, 15.4% for the second frequency, and 9.4% for the third frequency.

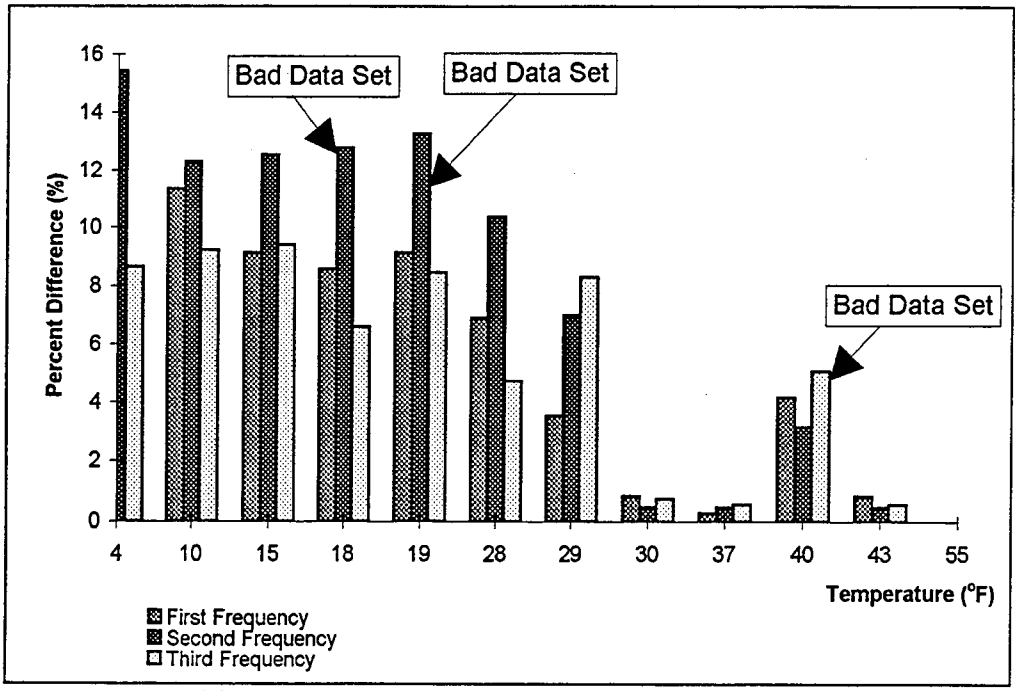

Figure 6 Percent Difference Change in Natural Frequency -from the Baseline Value

Modal Displacements

In order to demonstrate how the variation in temperature influences the normalized modal displacements, the three sets of data for the extreme temperatures are evaluated. They are listed in Table A2 in the Appendix. The data used correspond to 55°F and 10°F. The two baseline sets at 55°F are compared with each other, and then with the set at 10°F. The magnitude of the normalized modal displacements at the different acceleration sensor locations for the three sets of data are plotted in Figure 7. These do not show the actual mode shapes since the sensors are located over a two-dimensional grid. Nevertheless, this approach clearly shows the difference in the mode shapes. The data for sensors 5 and 11 are not plotted since these sensors were not functioning properly. As shown, there is little change in the modal displacements at different temperatures, except for that of the second bending mode.

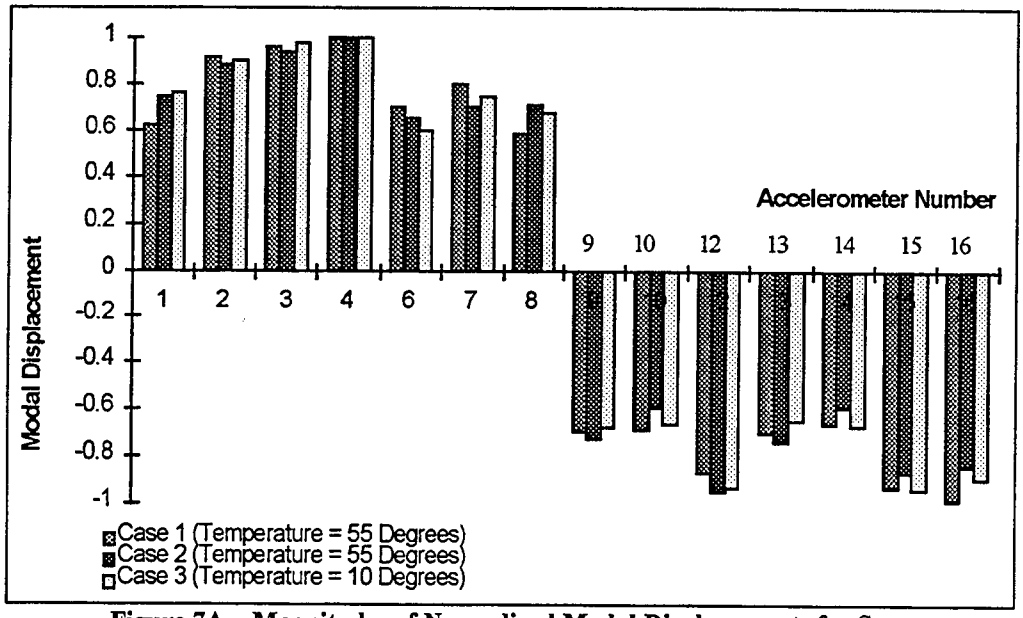

Figure 7A Magnitudes of Normalized Modal Displacements for Sensors
- First Bending Modal Displacements

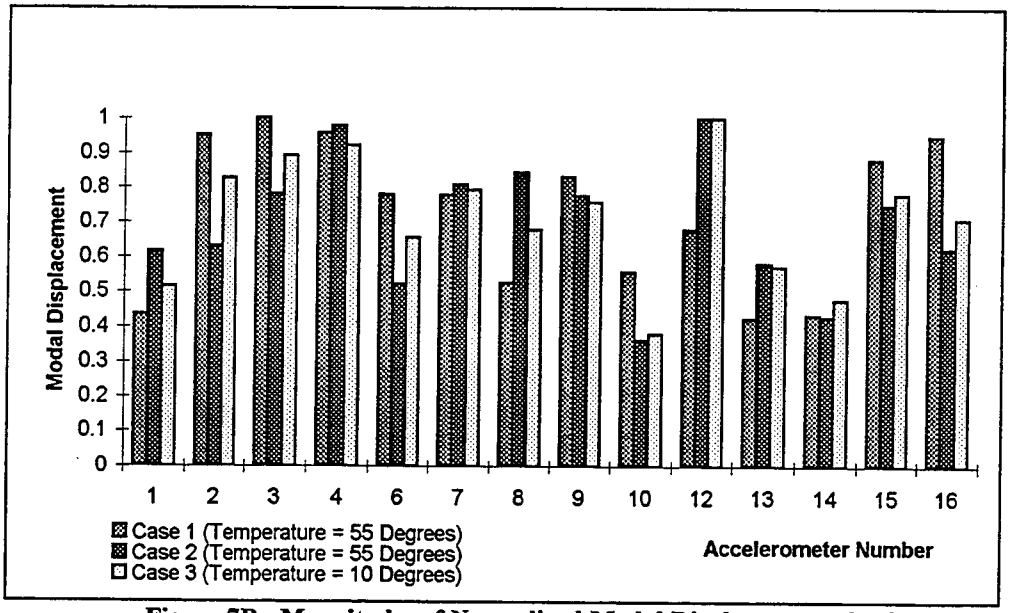

Figure 7B Magnitudes of Normalized Modal Displacements for Sensors
- Second Bending Modal Displacements

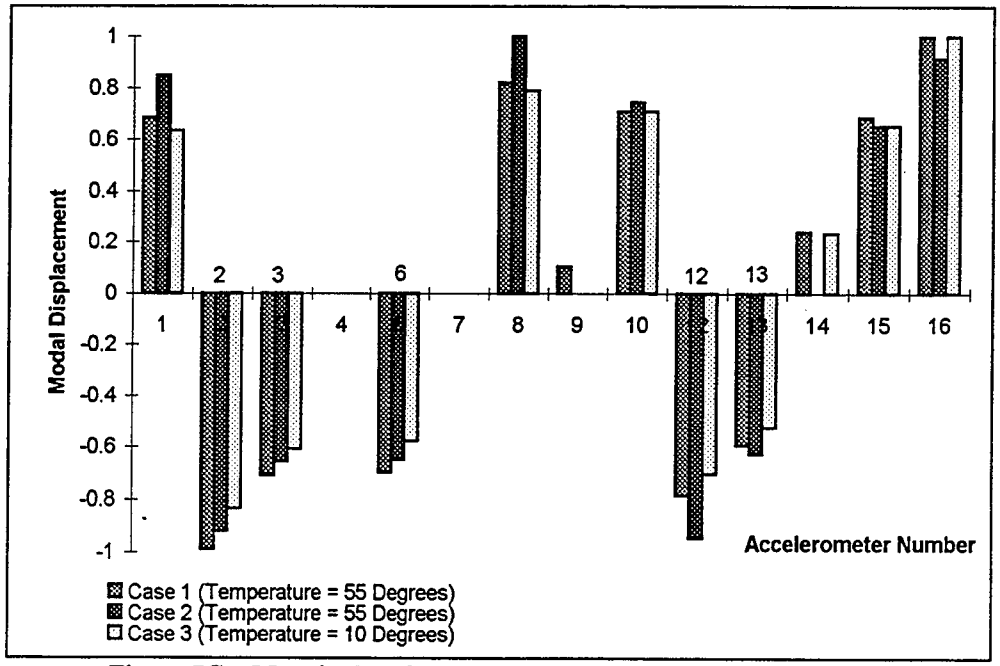

Figure 7C Magnitudes of Normalized Modal Displacements for Sensors
- First Torsion Modal Displacements

As a further comparison, Figure 8 shows the percent differences between case 1 and case 2 (same temperatures), and between case 1 and case 3 (different temperatures) for the data plotted in Figure 7. From these figures, no consistent trend is shown, even for case 1 and case 2, which have the same temperatures. As shown in Figure 8, the maximum values of the percent difference for the first bending, the first torsional and the second modal displacements are 22.0 % (between case 1 and 2), 100% (between case 1 and 2, and between case 1 and 3) and 60.8% (between case 1 and 2). The variations in the normalized modal displacements are as large at the same temperature (case 1 and 2) as at the different temperatures (case 1 and 3). These differences are due to variations in traffic loading for the different data sets.

Comparing the modal displacements at different temperatures, it is concluded that the modal displacements are unlikely to show changes in structural behavior of the bridge due to the temperature change.

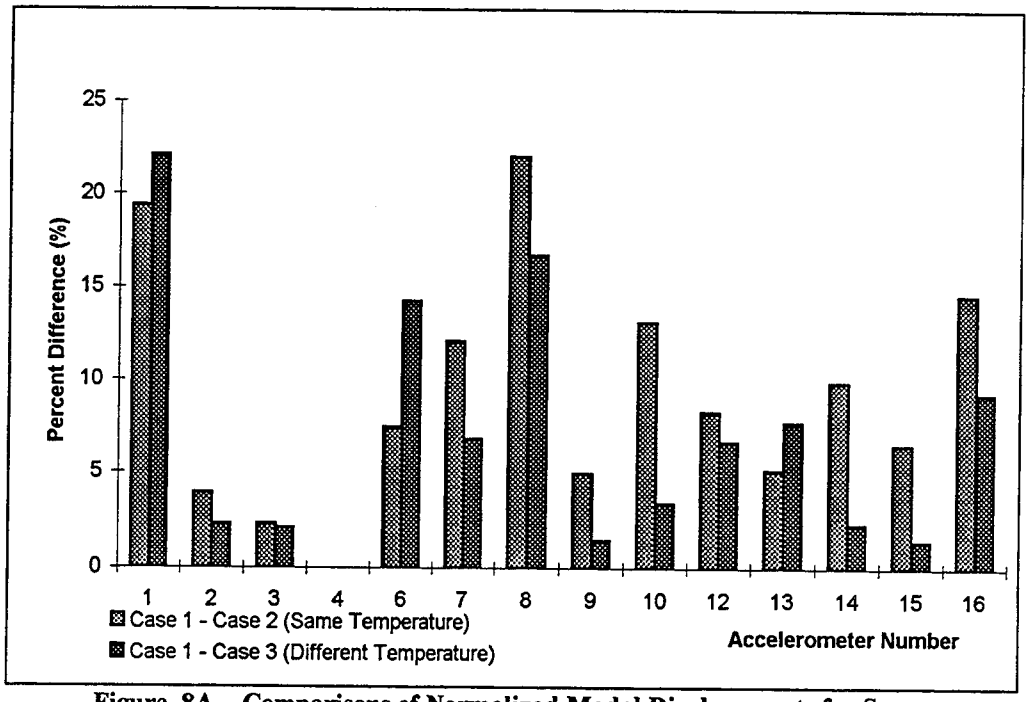

Figure 8A Comparisons of Normalized Modal Displacements for Sensors - First Bending Modal Displacements

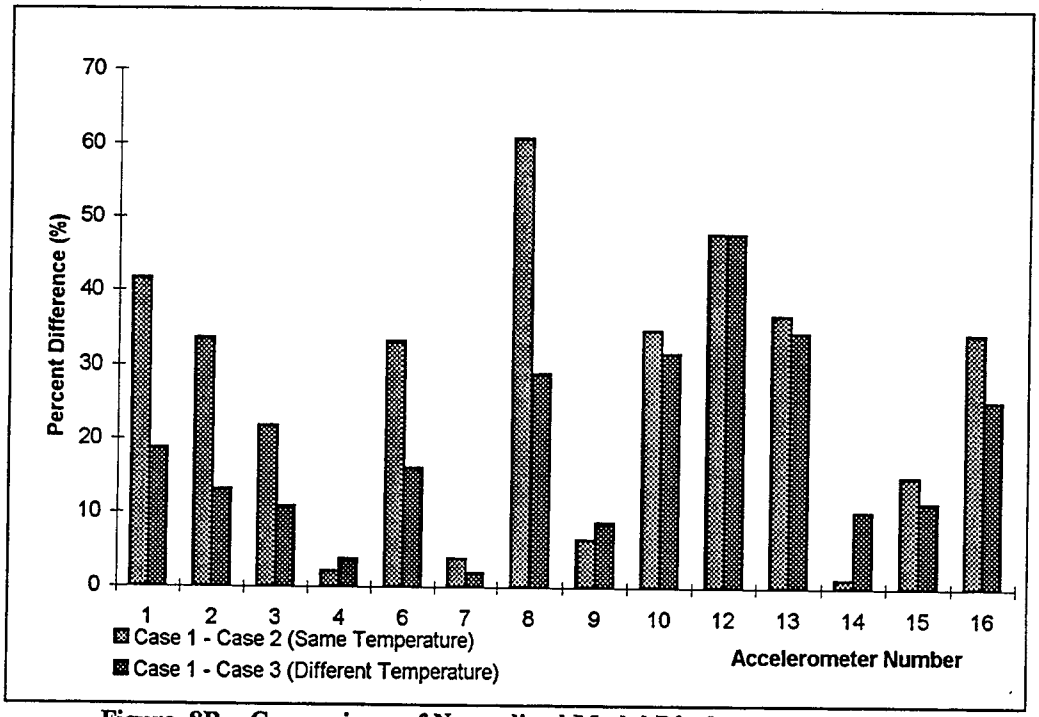

Figure 8B Comparisons of Normalized Modal Displacements for Sensors - Second Bending Modal Displacements

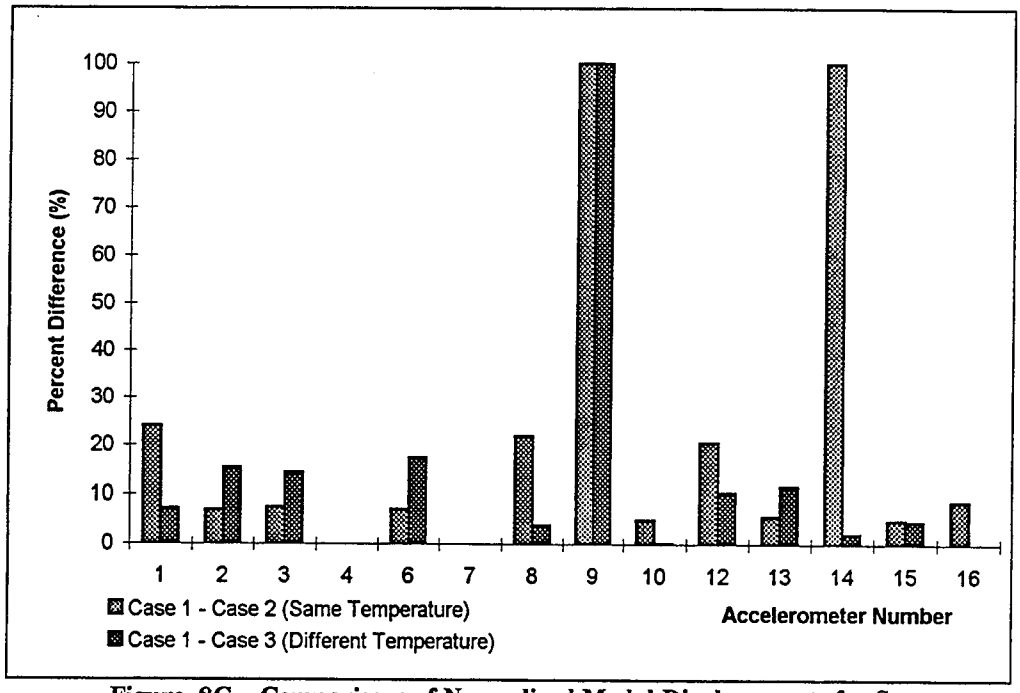

Figure 8C Comparisons of Normalized Modal Displacements for Sensors - First Torsion Modal Displacements

Modal Assurance Criterion (MAC)

The MAC is an alternative approach to the comparison of individual mode shapes. The MAC compares two modal displacements for different data sets at a specific natural frequency. The diagonal terms in the MAC dominate because of the orthogonal properties of modal displacements. Thus, the non-diagonal terms of the MAC matrix are smaller than the diagonal terms. Therefore, it should be only necessary to consider the diagonal terms. Modal displacements are compared to each other, such as the comparison between first modal displacements from two different sets of data. In this study, only the diagonal terms of the MAC are used in evaluating the structural behavior.

Table A3 in the Appendix lists the values of the MAC and the percent difference between the baselines at 55°F and the test data at different temperatures. Figure 9 shows the diagonal terms of the MAC, with legend of M_1, M_2 and M_3, excluding the bad data. These are based on a comparison of the values with baseline 1 at the temperature of 55°F. M_1, M_2, and M_3 individually represent the first, second and third diagonal terms of the MAC matrix. They relate the comparison of the first bending modal displacements, the first torsional modal displacements, and the second bending modal displacements with their corresponding baselines. Figure 9 indicates that the changes in the MAC are relatively small for the good data. The MAC comparisons show that the larger percent differences in the MAC occur for M_2. The maximum difference in this data occurs at M_2 with a value of 20.0% at the temperature of 4°F. This shows that the torsional mode shape is more sensitive to the restraint provided by the bearings as a result of the change in

temperature.

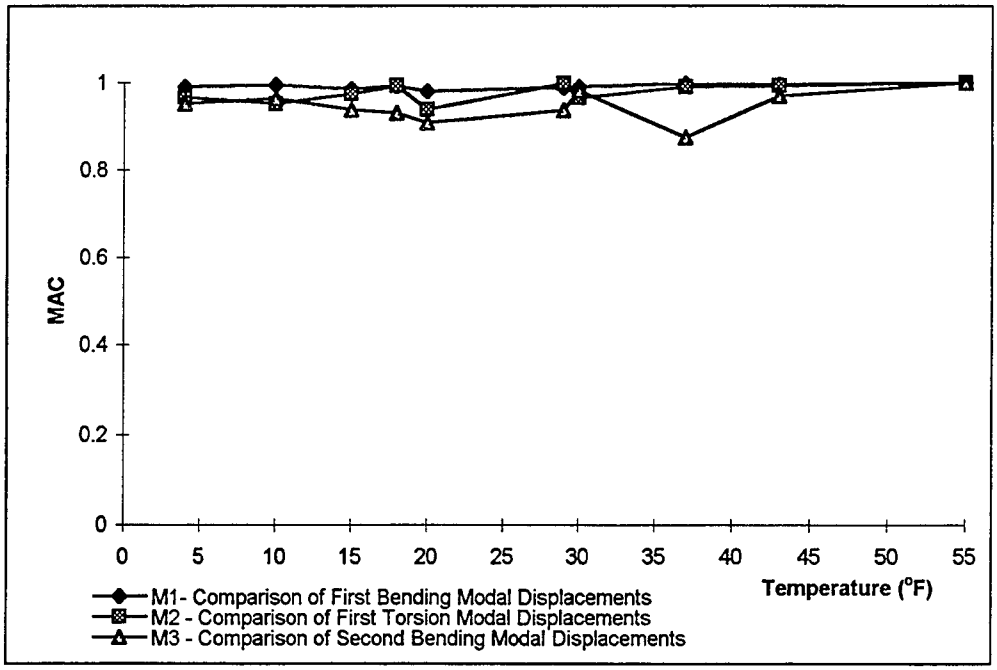

Figure 9 MAC Distribution Versus the Temperature (Without Bad Data) - Based on Baseline 1

As a further comparison, the bad data is included. This is done in Figure 10. The values for all 14 sets of data are at 12 different temperatures, including the bad data. These are done for the first and second baseline data sets at 55°F. As shown in this figure, M_1 does not change with a change in temperature. The largest changes occur for M_2 and M_3 for temperatures of 18°F, 19°F and 40°F, which are the temperatures associated with the bad data (these are for accelerometers 4, 6, 8 and 9, as shown in Figure 2). This confirms that those data are not acceptable. Changes in the structure should be noted more consistently over a wider temperature range.

The comparisons for the MAC provide a way to define the bad data sets. No consistent differences in the MAC occur based on the two different baselines, and thus it is unlikely that the MAC will clearly identify the changes in the structural behavior due to the changes in temperature.

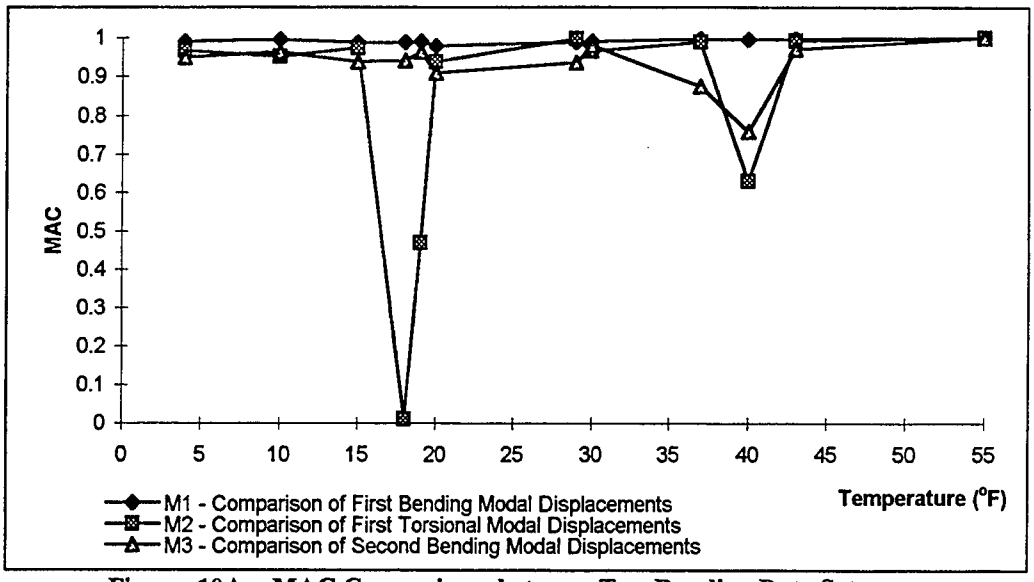

Figure 10A MAC Comparisons between Two Baseline Data Sets
- Based on Baseline 1

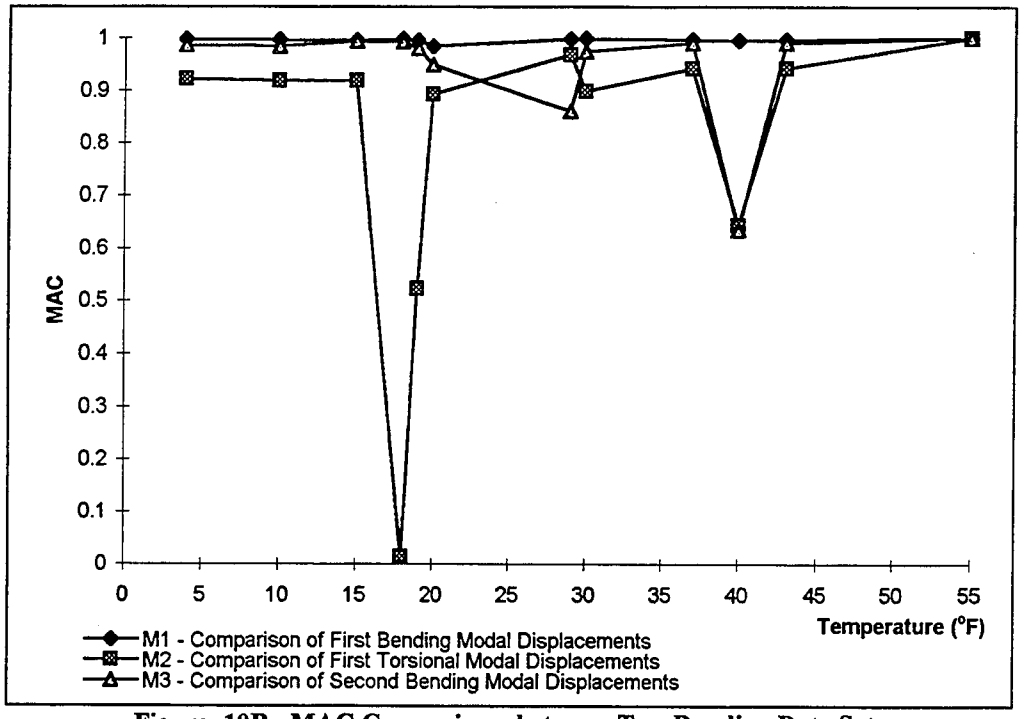

Figure 10B MAC Comparisons between Two Baseline Data Sets
- Based on Baseline 2

Coordinate Modal Assurance Criterion (COMAC)

Another approach to use modal displacements in bridge monitoring is the COMAC. The COMAC compares the response at a specific accelerometer from two

different data sets. Unlike the MAC, it evaluates the changes in structural integrity by comparing all mode shape magnitudes at a specific place on the structure. Table A4 and A5 in the Appendix list the values of COMAC and the percent difference in the COMAC at the different temperatures for all accelerometers when compared to the two different baseline temperatures of 55°. In order to find out the difference of using two baselines, the comparisons with the two different baseline data sets were done using the data from selected accelerometers 1, 2, 7, 9, 13, and 15. This selection includes three accelerometers for each span at the outer and inner parts in the transverse direction to reflect the structural global response of the bridge. The comparisons in the selection show that there is not a significant difference between the two COMAC evaluations using the two different baseline temperatures. Therefore it is not necessary to consider two baselines for the COMAC comparisons which follow.

Figures 11 and 12 show the plots of the COMAC for all accelerometer locations based on one of the two baseline temperatures of 55° for the different temperatures. Figure 11 does not include the bad data, and Figure 12 includes the bad data. According to the definition of the COMAC, the values below 1.0 indicate a change in the structural behavior.

For Figure 11, the values of the COMAC show little change. This is expected because the bad data is not included, and the COMAC should approach 1.0. For Figure 12, the COMAC has lower values at temperatures of 18°F, 19°F and 40°F, for which the data are bad.

Analysis with the COMAC does not clearly show that the structural stiffness changes due to temperature changes. It also does not provide a consistent indication of the changes in the structural behavior. However, it indicates which data sets are bad, as was shown with the MAC. This is different than the study by Lauzon (1997). In that study a cut was made in one of the girders. The cross signature assurance criterion (CSAC) evaluated at locations adjacent to the cut provided a significant indication of damage. The difference between the bridge in this study and that in the Lauzon's study is likely due to the difference in the types of modifications made to the structures. In Lauzon's study, the change was large and at a specific location, while in the bridge reported in this study, the relative change in behavior is smaller and distributed across the both ends.

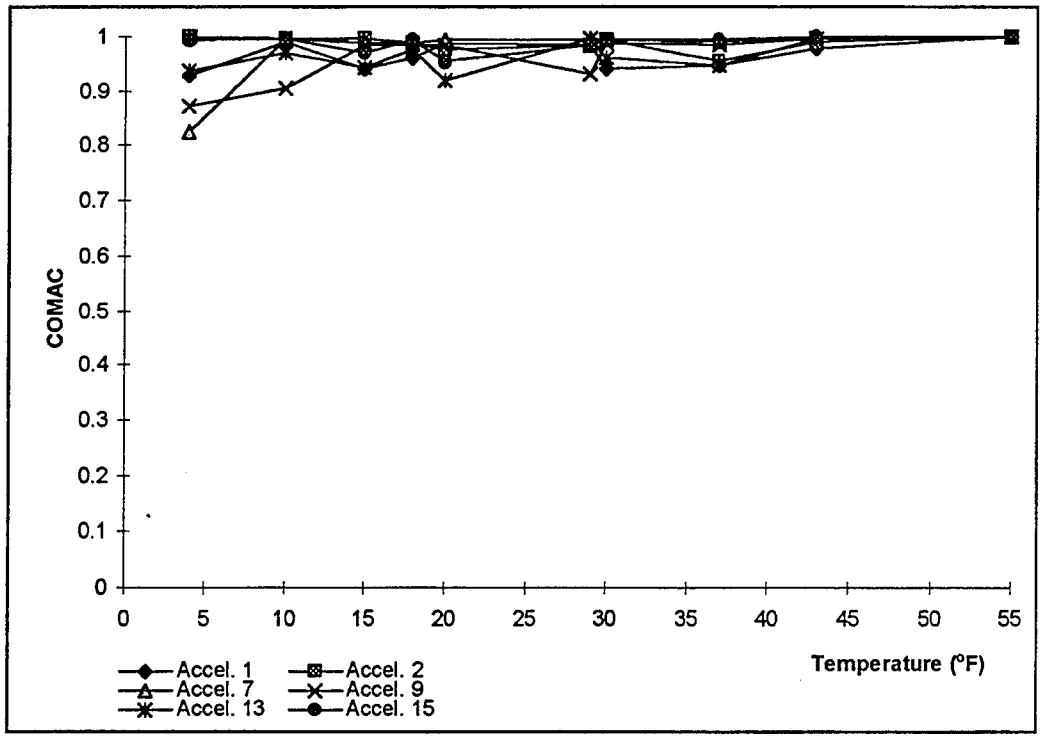

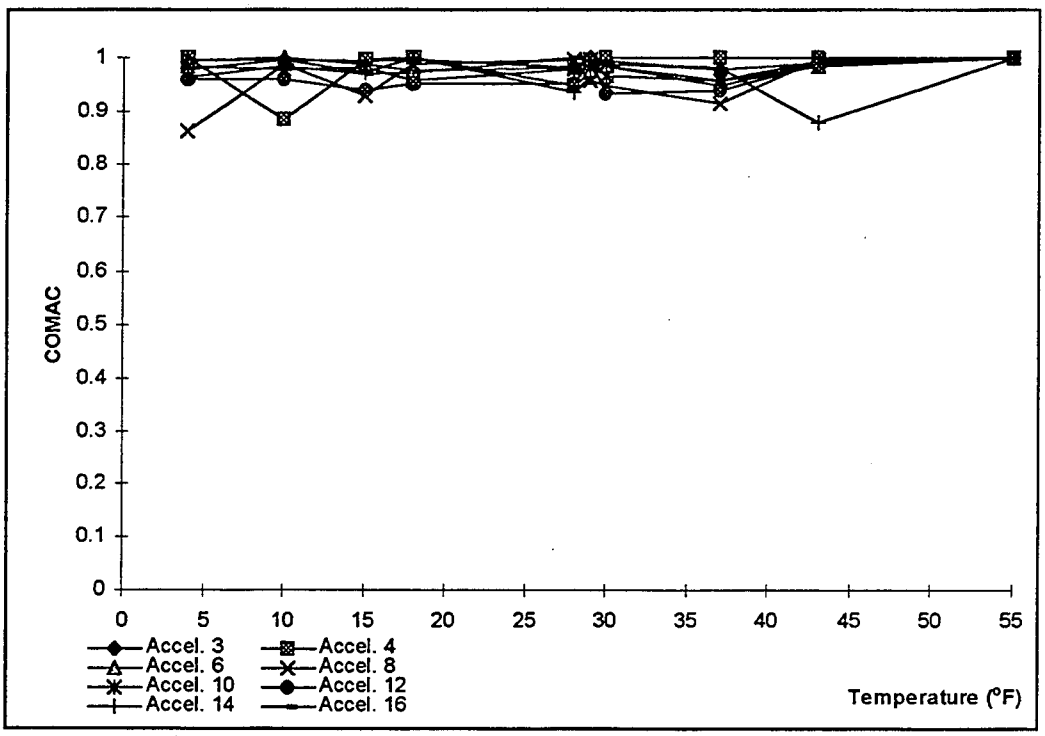

Figure 11 COMAC Comparisons - Without Bad data Included

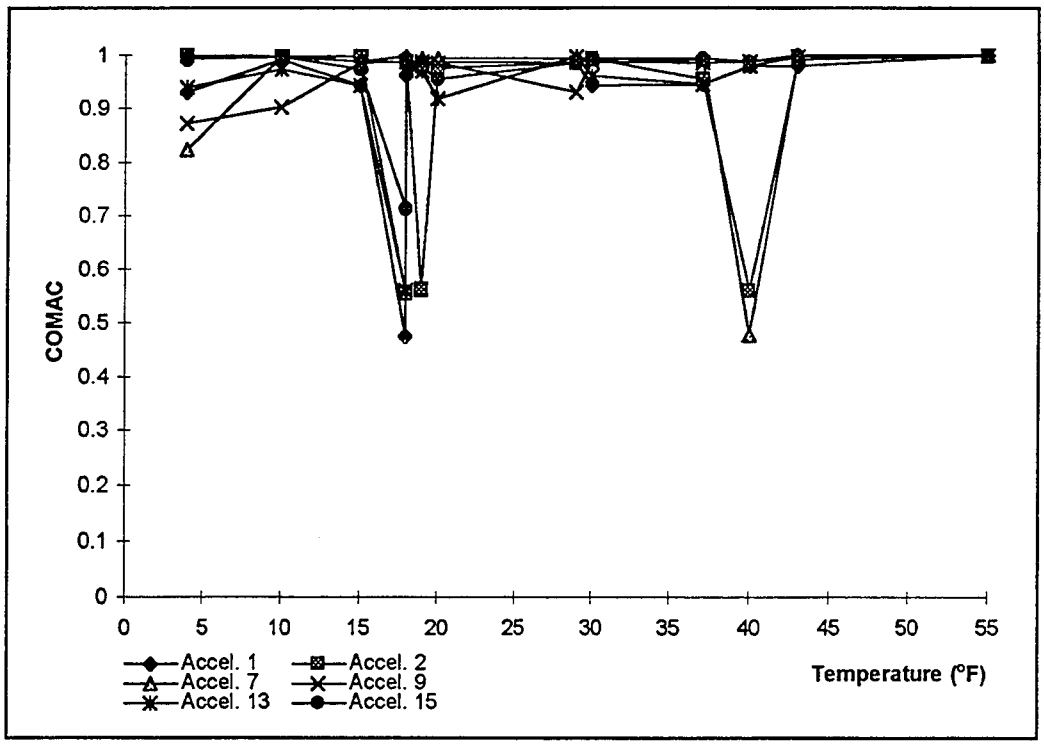

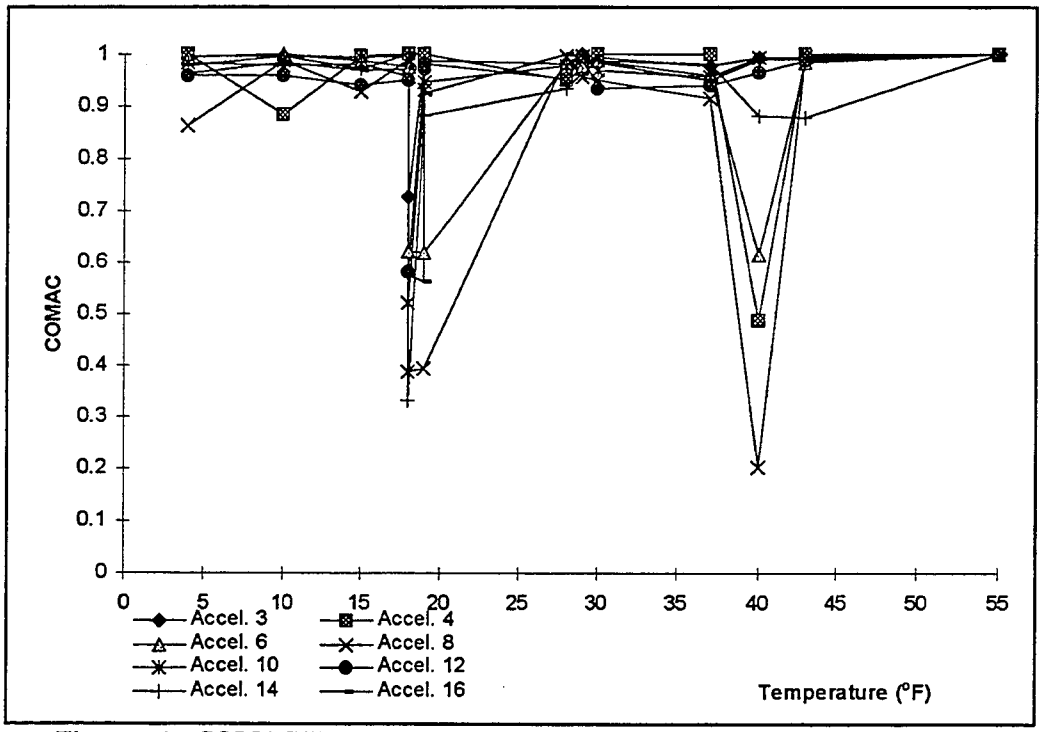

Figure 12 COMAC Versus the Temperature -With Bad Data Included

Modal Flexibility

The modal flexibility method is based on both the natural frequencies and unit mass modal displacements, and it is thus different than the MAC and COMAC. It is not possible to calculate the modal flexibility by its original definition for the bridge reported in this study. The problem is that the mass information is not available. Therefore the modal flexibility method is modified in this study so that only the modal displacements are required. This is done directly using the modal displacements as the mode shapes, [ϕ], of Equation (1). Mass information is not involved in the modal flexibility.

Initially, three sets of initial modal displacements and corresponding natural frequencies were directly used in Equation (1). Two sets of comparisons were made, one between the baseline temperature and 10°F and one between the two baseline temperatures. They are listed in Table A7 in the Appendix and shown in Figures 13A and B. This shows the comparisons of modal flexibility which are based on the diagonal terms in the modal flexibility matrix.

Figure 13A and B show that the modal flexibility is smaller for the lower temperature of 10°F. The percent difference in the diagonal terms of the modal flexibility between case 1 and case 2 (based on the same temperatures), as given in Table A7 in the Appendix, are 6.0%, 4.4% and 12.4%, and those between case 1 and case 3 (based on the different temperatures) are 20.8%, 34.1%, and 22.3%. In Figure 13, the small differences between the two baseline temperatures of 55°F may be due to variations in the field data in which the excitation from vehicular traffic varies.

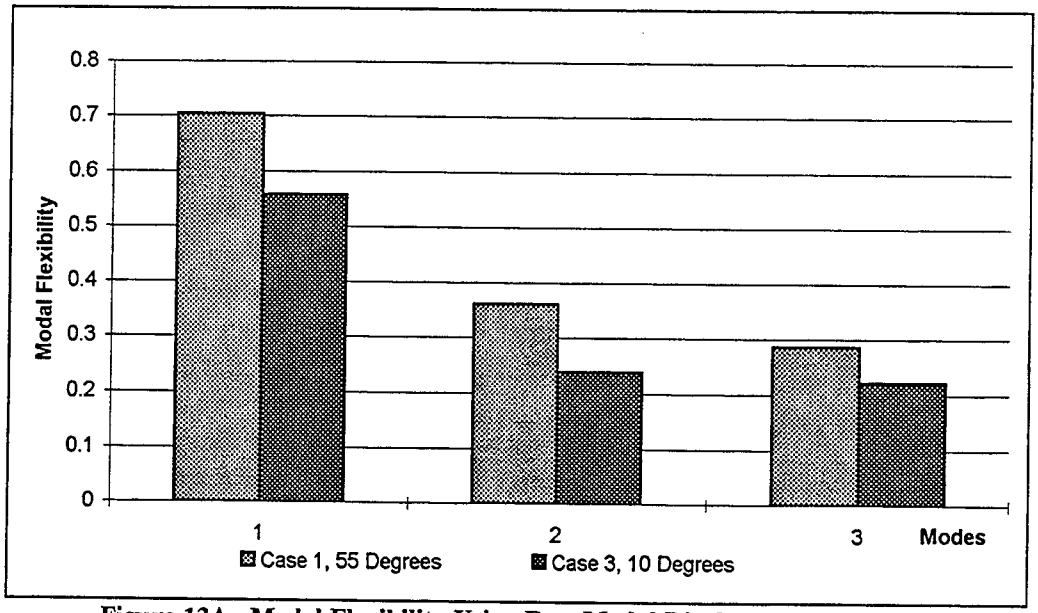

Figure 13A Modal Flexibility Using Raw Modal Displacements
Without Using Data Processing Approach - Case 1 and 3: Different Temperature

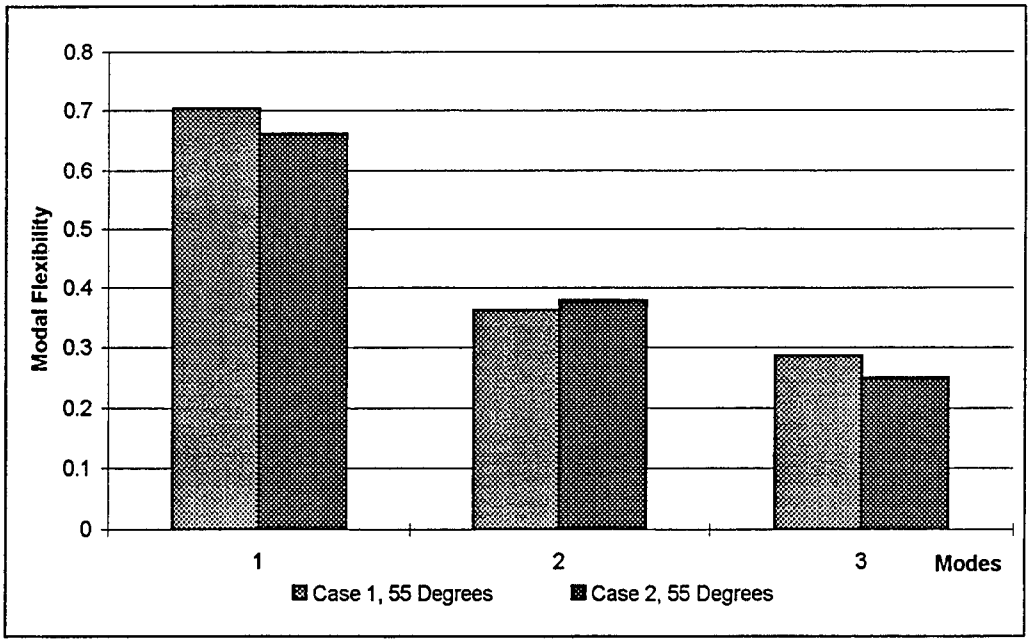

Figure 13B Modal Flexibility Using Raw Modal Displacements
Without Using Data Processing Approach - Case 1 and 2: Same Temperature

The modal flexibility thus produces significantly larger changes than are produced for the other approaches previously discussed. This is because the modal flexibility includes both the changes in the natural frequencies and corresponding modal displacements.

To reduce the variations in the two modal displacements at the same temperature and the modal displacements at different temperatures and to improve the results of the modal flexibility, a modification in the approach was made. The data processing approach which was found to be most effective was based on following equation:

$$\phi_i = \frac{\phi_i^0}{[\sum_{j=1}^{n} (\phi_j^0)^2]^{\frac{1}{2}}} \qquad (6)$$

where ϕ_i^0 = raw normalized modal displacements. A modal displacement vector processed with this approach results in a modal displacement vector with an unit length equal to the square root of the sum of the squares. As demonstrated in the following results using the modified modal flexibility, the changes in the structural behavior due to the change in temperature are still obvious. Additionally, the comparisons of the data at the same temperatures are much closer.

The initial modal displacements for same three sets of data which were used for

Figure 13 are processed with Equation (6). The resulting values are given in Table A7 in the Appendix. They are shown in Figure 14. The percent differences in the diagonal terms of modal flexibility between case 1 and case 2 (based on the same temperatures) are 2.2%, 1.9%, and 2.6%. Those between case 1 and case 3 (based on the different temperatures) are 20.2%, 22.1%, and 17.1%.

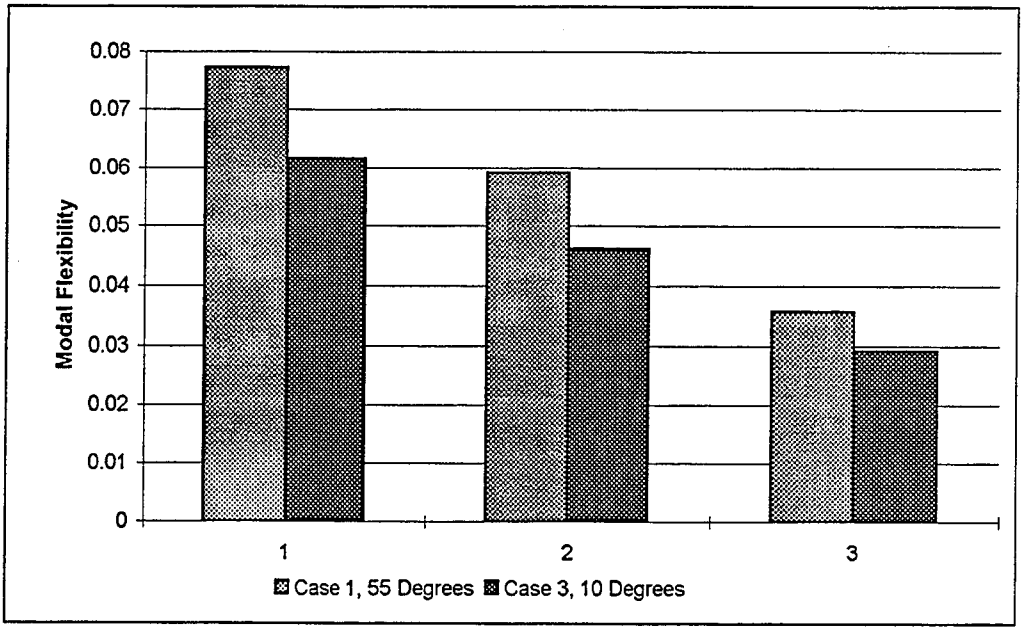

Figure 14A Modal Flexibility
Using Data Processing Approach - Case 1 and 3: Same Temperature

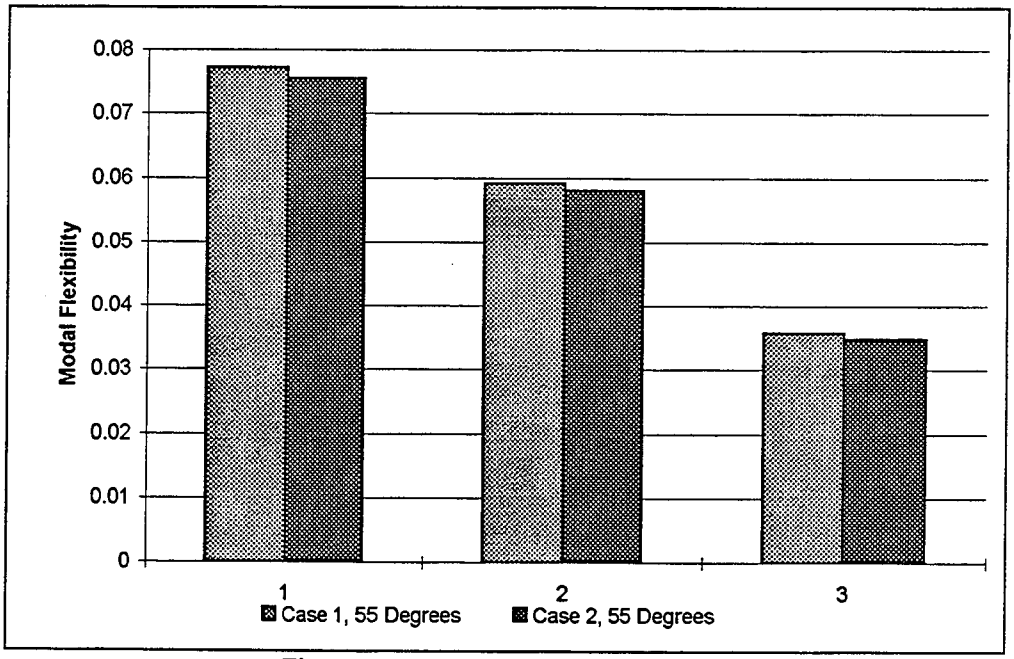

Figure 14B Modal Flexibility
Using Data Processing Approach - Case 1 and 2: Different Temperature

Figure 14A and B still show obvious differences in the modal flexibilities for case 1 and 3 at different temperatures. However, there is a much smaller difference in values of the data at the same temperature with the modified modal flexibility method. The comparison with different temperatures produces smaller changes, but still with significant values.

The modified modal flexibility method, with modal displacements modified using Equation (6) so that they are not based on the unknown mass matrix, are used now for all sets of data. The modal flexibility and the percent difference compared to the two baseline temperatures are given in Table A8 in the Appendix. Figure 15 plots the diagonal terms of the modal flexibility versus the difference in temperatures for the two separate baselines, based on the data in Table A8 in the Appendix which includes the bad data. There are very small differences in the results using the two different baselines. Additionally, this figure shows that the modal flexibility increases gradually as the temperature increases, except at the temperatures of 19°F and 40°F. As noted previously, the lower temperature produces partial restraint in the end bearings, and this results in the lower values in the modal flexibility.

Figure 16 shows the percent difference between the baseline and the test data using the values in Table A8 for the different temperatures. The maximum percent difference in modal flexibility is 24.2%. This occurs at F_2, which is related to the first torsional mode shape. As expected there is no significant difference in the results using either of the baseline temperatures. The MAC and COMAC did not show as large a difference due to temperature changes as the modal flexibility did. The modal flexibility shows changes at all different temperatures below the baseline values. As noted earlier, this is because the modal flexibility involves both the modal displacements and the natural frequencies which are influenced by the changes in temperature.

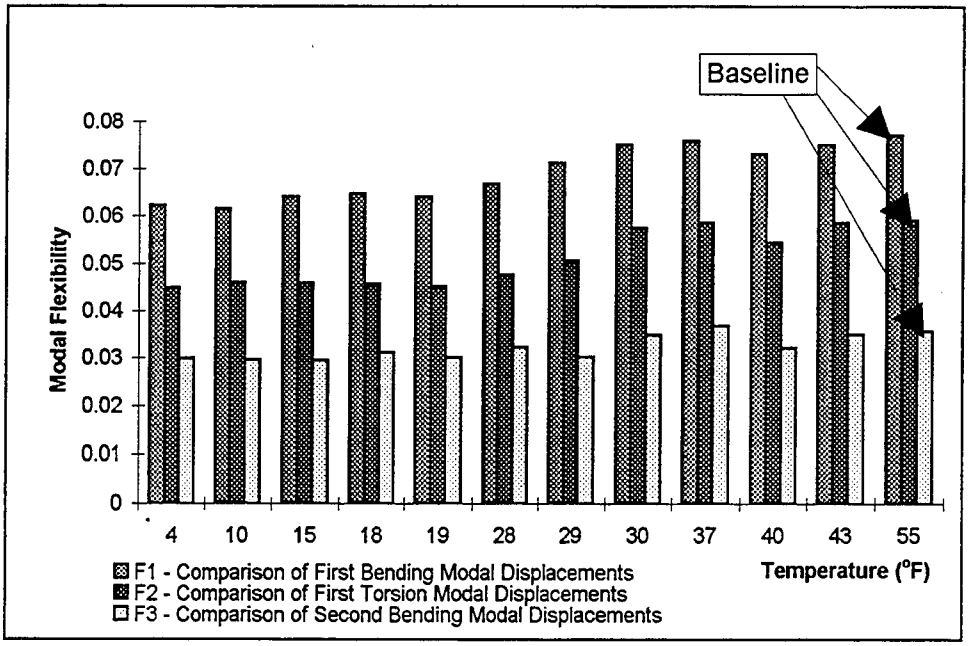

Figure 15A Modal Flexibility Distribution Versus Temperature
All Data Included - Based on Baseline 1

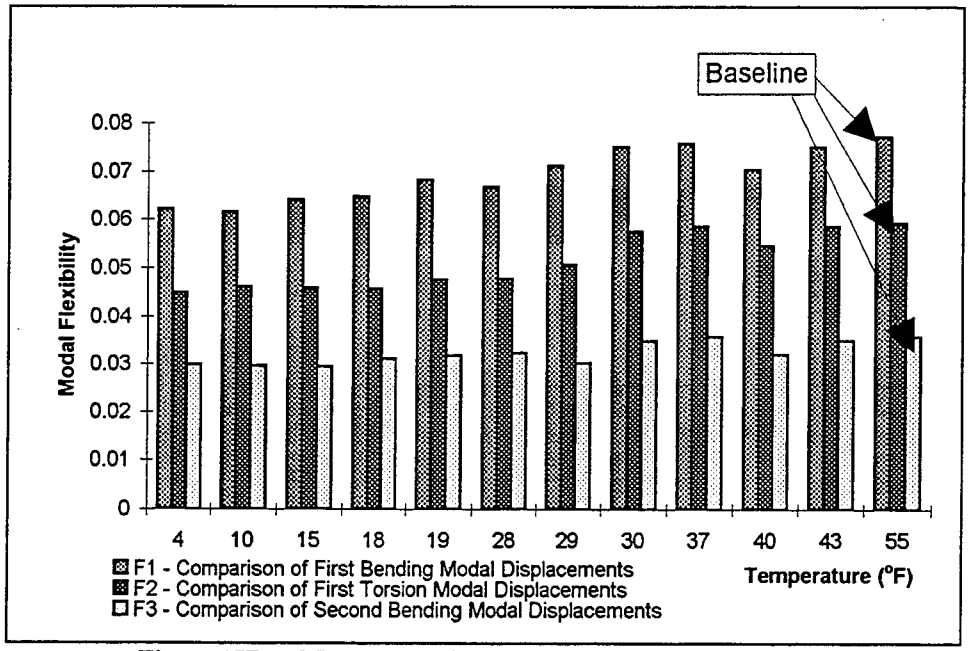

Figure 15B Modal Flexibility Distribution Versus Temperature
All Data Included - Based on Baseline 2

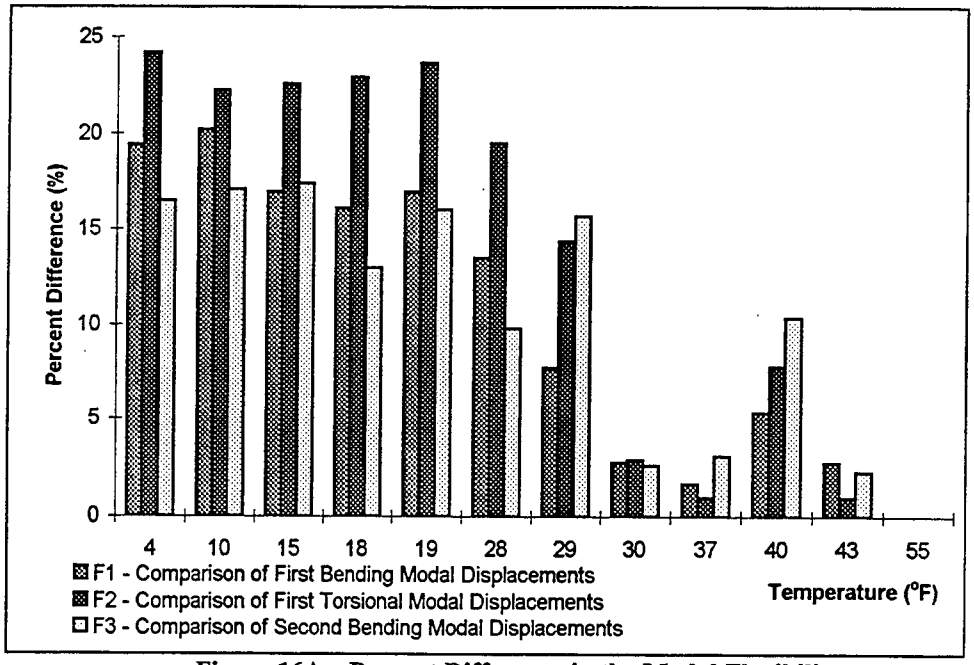

Figure 16A Percent Difference in the Modal Flexibility
All Data Included - Based on Baseline 1

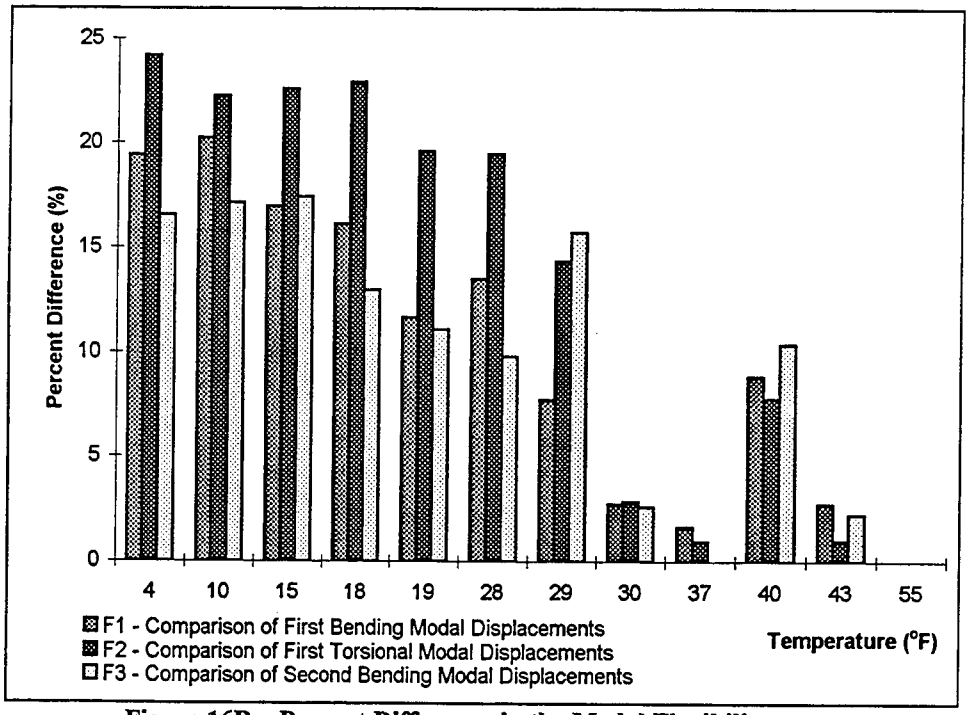

Figure 16B Percent Difference in the Modal Flexibility
All Data Included - Based on Baseline 2

CONCLUSIONS

The use of normal traffic for load excitation in bridge monitoring is a promising method. It can be applied to remote monitoring, and it can be used continuously because it does not require interruptions to traffic.

The traditional dynamic properties of bridges, natural frequencies and modal displacements and their derivatives, including the modal assurance criterion, the coordinate modal assurance criterion, and the modal flexibility, can be useful diagnostic parameters in bridge evaluations. In this study the natural frequencies and modal displacements were determined using fast Fourier transform to obtain the frequency spectrum from the accelerations. The results were found to vary with changes in temperature below approximately 60°F. This was due to partial restraint in the expansion bearings.

Specific conclusions are as follows:

1). The changes in the structural integrity at different temperatures, due to partial restraint of the expansion bearings, may be identifiable using natural frequencies and modal flexibility.

2). A method is developed for eliminating the bad data sets. This is done by checking if the modal displacements are reasonable, which means that they can be readily defined. This was shown with the modal assurance criterion and the coordinate modal assurance criterion approaches. The bad data should not be used for the evaluation of the bridge because the changes due to the bad data are larger than due to the changes in the structural stiffness.

3). The modal flexibility method may be applied using mode shapes, or modal displacements when mass information is not available.

4). Based on the calculation of the percent difference between the baselines at 55°F and the test data at lower temperatures, the followings are observed:

a. Natural frequencies can be used to determine changes in bridges due to changes in temperature. The maximum percent difference was 15.4% for the temperature of 4°F. This occurred at the natural frequency associated with the first torsional mode.

b. Modal displacements are not good indicators when used alone.

c. The modal assurance criterion is better suited for global structural integrity evaluations than modal displacements. The maximum percent difference in the

modal assurance criterion was 20.0% for the temperature of 4°F.

d. The coordinate modal assurance criterion often provides indication of local changes in structures. It was not successful in this study, in which the changes in structural integrity are global. The maximum percent difference in the coordinate modal assurance was 17.6% for the temperature of 4°F.

e. The modal flexibility provided the best evaluation of the changes in the structural behavior. The changes were the largest, with the maximum percent difference equal to 26.4% for the temperature of 4°F.

Bridge monitoring and health evaluation requires more specific care when the excitation is with vehicular traffic than when the excitation can be determined, such as when using impact hammers and hydraulic actuators. There are variations in the response of the bridge due to the weight, speed, and vehicle lane position. The application of natural frequencies, modal displacements, the modal assurance criterion, the coordinate modal assurance criterion and the modal flexibility have been used in this study.

The writers feel that the use of a combination of these methods will typically produce more reliable results than use of any single method.

REFERENCES

Alampalli, S., and Fu, Gongkang (1992). "Sensitivity of On-Line Modal Property Identification For Bridge Inspection." Third NSF Workshop on Bridge, Engineering Research in Progress, LaJolla, CA November 16-17,1992.

Alampalli, S, Fu, G. and Dillon, E. W. (1995). "Measuring Bridge Vibration for Detection of Structural Damage." Report FHWA/RR-95/165.

Aktan, A.E. and et. (1995). "Field Laboratory for Modal Analysis and Condition Assessment of Highway Bridges." North American Workshop on Instrumentation and Vibration Analysis of Highway Bridges, Cincinnati, Ohio.

Aktan, A. E., Lee, L. and Dalal, V. (1995). "Multireference Modal testing for Bridge Diagnostics." North American Workshop on Instrumentation and Vibration Analysis of Highway Bridges, Cincinnati, Ohio.

Chang, K. C., Shen, Z. and Lee, G. C. (1993). "Mode Analysis Technique for Bridge Damage Detection." Natural Hazards Mitigation.

Chen, S. S. and Kim S. (1995). " Neural Network Based Monitoring of Instrumented Structures." Restructuring: America and Beyond, Proceedings of Structures Congress XIII, Boston, MA, 1995.

Conn, P. E. (1994). "Monitoring The Vibration of A Continuous Bridge." M. S. Thesis, University of Connecticut.

Conn, P. E. and DeWolf, J . T. (1995). "Vibrational Behavior Of A Continuous Span Bridge." Department of Civil Engineering Report.

DeWolf, J. T. and Fu, Yongda (1997). "Evaluation of Temperature Induced Changes in A Multigirder Steel Two-Span Bridge." Technical Report to Connecticut Department of Transportation, June 1997.

DeWolf, J. T., Conn, P. E. and O'Leary, P.N. (1995). "Continuous Monitoring Of Bridge Structures." IABSE Symposium, San Francisco, CA 1995.

Fu, Yongda (1996). "Analytical Evaluation of Experimental Bridge Vibratio Behavior." Master Thesis, University of Connecticut.

Halvorsen, W. G. and Brown, D L. (1995). "Impact Technique for Structural Frequency Response Testing." North American Workshop on Instrumentation and Vibration Analysis of Highway Bridges, Cincinnati, Ohio.

Kim, Jeong-Tae and Stubbs, N. (1995). "Model-Uncertainty Impact and Damage-Detection Accuracy in Plate Girder." J. of Structural Engineering, Vol. 121, No. 10.

Law, S.S., Ward, H. S., Shi, G.B., Chen R. Z., Waldron, P. and Taylor,C. (1995). "Dynamic Assessment of Bridge Load-Carrying Capacities." J. of Structural Engineering, Vol. 121, No. 3.

Lauzon, R. G. (1997). "Vibrational Monitoring of A Full-Scale Highway Bridge Undergoing A Destructive Test." Ph.D. Thesis, University of Connecticut, 1997.

Lauzon, R. G. and DeWolf, J. T. (1996). "Nondestructive Evaluation With Vibrational Analysis." Nondestructive Testing Methods For Civil Infrastructure, ASCE, Boston, MA.

Lauzon, R. G. (1995). " Full-Scale Bridge Testing to Monitor Vibrational Signatures: Phase II Major Structure Investigation." Interim Report, Report 1408-2-95-5, Connecticut Department of Transportation.

Lauzon, R. G. and DeWolf, J. T. (1993). " Full-scale Bridge Test to Monitor Vibrational Signatures". Structural Engineering in Natural Hazards Mitigation, Irvine, CA, April 19-21, 1993, ASCE.

Mazurek, D. F. and DeWolf, J. T. (1990). "Experimental Study of Bridge Monitoring Technique." J. of Structural Engineering, ASCE, 116(9).

Raghavendrachar, M. and Aktan, A. E. (1992) "Flexibility by Multireference Impact Testing for Bridge Diagnostics." J. of Structural Engineering, Vol. 118, No. 8, August.

Sartor, R. R., DeWolf, J. T. (1996). "Cracking In Connections Between Floorbeams And Supporting Girders - Developing And Use Of A Portable Strain Monitoring System For Bridge Evaluations." JHR 96-246, report, Project 92-2.

Shelley, S.J. (1995) "Dynamic Testing (Vibration Analysis) of Highway Bridge." North American Workshop on Instrumentation and Vibration Analysis of Highway Bridges, Cincinnati, Ohio.

Shelley, S. J., Lee, K. L., Aksel, T. and Aktan, A. E. (1995). " Active-Control and Forced- Vibration Studies on Highway Bridge." J. of Structural Engineering, Vol. 121, No. 9.

Shen, Stuart S. and Kim, S. (1995). "Neural Network Based Sensor Signal Monitoring of Instrumented Structures." Restructuring: America and Beyond Proceedings of Structures Congress XII, Boston, MA, April 2-5, 1995.

Stubbs, N. and Sikorsky, C. S. (1995). "General Methodology to Evaluate Bridge Structural Safety." North American Workshop on Instrumentation and Vibration Analysis of Highway Bridges, Cincinnati, Ohio.

Toksoy, T. and Aktan, A.E. (1995). "Bridge-Condition Assessment by Modal flexibility." North American Workshop on Instrumentation and Vibration Analysis of Highway Bridges, Cincinnati, Ohio.

APPENDIX

Table A1. Raw Data of Accelerations and Natural Frequency

Note: Temperature (F), Frequency (Hz)

	Data Set Number							
	1	2	3	4	5	6	7	8
Temperature (F°)	55	55	43	37	30	29	28	18
1st Frequency	3.6	3.64	3.65	3.63	3.65	3.747	3.87	3.93
2nd Frequency	4.11	4.19	4.13	4.13	4.17	4.44	4.58	4.67
3rd Frequency	5.29	5.36	5.35	5.29	5.36	5.761	5.57	5.71
Accelerometer Number	First Bending Modal Displacements							
1	0.652	0.746	0.764	0.742	0.783	0.793	0.707	0.759
2	0.918	0.882	0.898	0.932	0.861	0.857	0.791	0.835
3	0.959	0.937	0.95	0.982	0.952	0.912	0.901	0.937
4	1	1	0.992	1	1	0.958	1	1
6	0.703	0.651	0.644	0.664	0.622	0.604	0.575	0.544
7	0.797	0.701	0.735	0.763	0.739	0.705	0.749	0.757
8	0.582	0.71	0.703	0.685	0.73	0.761	0.599	0.655
9	-0.69	-0.724	-0.74	-0.705	-0.704	-0.734	-0.763	-0.745
10	-0.681	-0.592	-0.63	-0.67	-0.582	-0.645	-0.654	-0.611
12	-0.873	-0.945	-1	-0.956	-0.983	-1	-0.967	-0.964
13	-0.703	-0.739	-0.715	-0.673	-0.671	-0.764	-0.967	-0.774
14	-0.658	-0.593	-0.658	-0.699	-0.621	-0.616	-0.691	-0.627
15	-0.929	-0.869	-0.908	-0.982	-0.855	-0.873	-0.671	-0.864
16	-0.984	-0.841	-0.885	-0.936	-0.858	-0.894	-0.937	-0.8
	First Torsional Modal Displacements							
1	0.683	0.847	0.558	0.545	0.471	0.603	0.587	0.722
2	-0.987	-0.919	-1	-1	-0.985	-0.896	-1	-0.884
3	-0.71	-0.657	-0.714	-0.73	-0.782	-0.637	-0.786	-0.678
4	0	0	0	0	0	0	0.265	0.568
6	-0.698	-0.649	-0.738	-0.722	-0.761	-0.627	-0.657	-0.627
7	0	0	0	0	0	0	0	0.462
8	0.82	1	0.768	0.688	0.614	0.802	0.75	0.899
9	0.103	0	0	0	0	0.138	0	0.446
10	0.707	0.742	0.653	0.745	0.752	0.685	0.797	0.72
12	-0.783	-0.944	-0.66	-0.718	-0.5	-0.732	-0.614	-0.867
13	-0.592	-0.625	-0.49	-0.507	-0.386	-0.542	-0.614	-0.65
14	0.239	0	0.218	0.327	0.292	0.235	0.48	647
15	0.683	0.65	0.642	0.716	0.699	0.698	0.278	0.803
16	1	0.914	0.939	0.95	1	1	0.864	1
	Second Bending Modal Displacements							
1	0.435	0.616	0.638	0.573	0.525	0.363	0.499	0.69
2	0.951	0.632	0.899	0.506	0.838	1	0.693	0.739
3	1	0.783	0.889	0.657	0.945	0.785	0.843	0.867
4	0.958	0.978	0.991	0.842	1	0.565	1	1
6	0.781	0.522	0.752	0.444	0.721	0.825	0.569	0.604
7	0.779	0.809	0.856	0.766	0.841	0.508	0.86	0.875
8	0.525	0.844	0.812	0.799	0.653	0.761	0.59	0.893
9	0.83	0.777	0.783	0.786	0.808	0.451	0.829	0.971
10	0.556	0.363	0.489	0.28	0.393	0.522	0.445	0.444
12	0.677	1	1	1	0.861	0.618	0.97	0.988
13	0.425	0.581	0.551	0.58	0.487	0.376	0.97	0.695
14	0.433	0.428	0.423	0.5	0.42	0.223	0.551	0.511
15	0.88	0.749	0.827	0.69	0.802	0.603	0.465	0.821
16	0.948	0.623	0.914	0.447	0.755	0.924	0.849	0.823

Table A1. (Continued)

	Data Set Number							
	9	10	11	12	13	14	15	16
Temperature (F°)	18	15	10	4	4	19	19	40
1st Frequency	3.93	3.95	4.03	4.01	4.04	3.95	3.83	3.77
2nd Frequency	4.68	4.67	4.66	4.72	4.79	4.7	4.58	4.28
3rd Frequency	5.67	5.82	5.81	5.79	5.78	5.77	5.61	5.588
Accelerometer Number	First Bending Modal Displacements							
1	0.777	0.782	0.763	0.773	0.777	0.735	0.741	0.637
2	0.848	0.853	0.897	0.837	0.77	0.838	0.799	0.772
3	0.922	0.888	0.979	0.923	0.876	0.887	0.92	0.807
4	1	0.916	1	0.987	0.983	1	1	0.82
6	0.607	0.55	0.603	0.555	0.498	0.508	0.534	0.538
7	0.725	0.686	0.743	0.758	0.778	0.64	0.754	0.638
8	0.693	0.705	0.679	0.689	0.716	0.645	0.624	0.544
9	-0.738	-0.645	-0.68	-0.67	-0.738	-0.665	-0.72	-0.536
10	-0.598	-0.603	-0.658	-0.614	-0.615	-0.677	-0.609	-0.542
12	-0.984	-1	-0.931	-1	-1	-0.934	-0.929	-0.738
13	-0.723	-0.677	-0.649	-0.714	-0.749	-0.757	-0.706	-0.496
14	-0.645	-0.677	-0.673	-0.588	-0.639	-0.58	-0.638	-0.518
15	-0.892	-0.9	-0.942	-0.902	-0.879	-0.872	-0.878	-0.734
16	-0.86	-0.814	-0.893	-0.854	-0.847	-0.91	-0.865	-0.727
	First Torsional Modal Displacements							
1	0.592	0.516	0.643	0.554	0.479	0.427	0.866	0.182
2	-0.974	-0.825	-0.835	-0.949	-0.872	0	0	0
3	-0.71	-0.656	-0.608	-0.708	-0.746	-0.568	-0.668	-0.194
4	0	0	0.403	0	0.599	0	0	0
6	-0.694	-0.609	-0.577	-0.638	-0.645	0	0	0
7	0	0	0	0.365	0.451	0	0	0
8	0.768	0.653	0.789	0.701	0.676	0	0	0
9	0	0	0.379	0	0.48	0	0	0
10	0.679	0.725	0.708	0.711	0.696	0.644	0.721	0.192
12	-0.643	-0.547	-0.702	-0.664	-0.631	-0.51	-1	-0.28
13	-0.493	-0.413	-0.523	-0.468	-0.42	-0.378	-0.712	-0.158
14	0.247	0.341	0.234	0.308	0.354	0	0	0
15	0.716	0.777	0.652	0.641	0.663	0.574	0.699	0.191
16	1	1	1	1	1	1	0	0.259
	Second Bending Modal Displacements							
1	0.634	0.675	0.516	0.562	0.525	0.569	0.543	0.163
2	0.732	0.796	0.827	0.844	0.792	0.891	0.787	0.363
3	0.873	0.861	0.892	0.925	0.895	0.943	0.922	0.334
4	0.978	1	0.922	1	1	1	1	0
6	0.544	0.601	0.656	0.646	0.58	0.665	0.599	0.293
7	0.865	0.865	0.794	0.834	0.815	0.884	0.86	0
8	0.829	0.881	0.677	0.715	0.721	0.602	0.592	0
9	0.82	0.721	0.758	0.788	0.766	0.803	0.882	0.255
10	0.293	0.454	0.38	0.414	0.332	0.397	0.331	0.201
12	1	0.987	1	0.991	0.858	0.974	0.913	0.353
13	0.549	0.625	0.571	0.577	0.555	0.606	0.519	0.164
14	0.436	0.412	0.477	0.399	0.338	0.456	0.444	0.155
15	0.765	0.733	0.78	0.692	0.675	0.806	0.772	0.273
16	0.629	0.702	0.709	0.594	0.541	0.751	0.657	0.358

Note: shade data is not good, as discussed in the text.

Table A2. Modal displacements and Natural Frequencies

Case	1: Baseline 1: T=55°			2: Baseline 2: T=55°			3: Test Data: T=10°		
	Frequencies: F1=3.60 Hz			Frequencies: F1=3.64 Hz			Frequencies:F1=4.03 Hz		
	F2=4.11 Hz, F3=5.29 Hz			F2=4.19 Hz, F3=5.36 Hz			F2=4.66 Hz,F3=5.81 Hz		
Channel No.	Acceleration			Acceleration			Acceleration		
	B1	T1	B2	B1	T1	B2	B1	T1	B2
1	0.625	0.683	0.435	0.746	0.847	0.616	0.763	0.634	0.516
2	0.918	-0.987	0.951	0.882	-0.919	0.632	0.897	-0.835	0.827
3	0.959	-0.710	1.000	0.937	-0.657	0.783	0.979	-0.608	0.892
4	1.000	0.000	0.958	1.000	0.000	0.978	1.000	0.000	0.922
6	0.703	-0.698	0.781	0.651	-0.649	0.522	0.603	-0.577	0.656
7	0.797	0.000	0.779	0.701	0.000	0.809	0.743	0.000	0.794
8	0.582	0.820	0.525	0.710	1.000	0.844	0.679	0.789	0.677
9	-0.690	0.103	0.830	-0.724	0.000	0.777	-0.680	0.000	0.758
10	-0.681	0.707	0.556	-0.592	0.742	0.363	-0.658	0.708	0.380
12	-0.873	-0.783	0.677	-0.945	-0.944	1.000	-0.931	-0.702	1.000
13	-0.703	-0.592	0.425	-0.739	-0.625	0.581	-0.649	-0.523	0.571
14	-0.658	0.239	0.433	-0.593	0.000	0.428	-0.673	0.234	0.477
15	-0.929	0.683	0.880	-0.869	0.650	0.749	-0.942	0.652	0.780
16	-0.984	1.000	0.948	-0.841	0.914	0.623	-0.893	1.000	0.709

Note: B1, B2 = first and second bending modal displacements, respectively; T1 = first torsional mode shape.

Table A3. MAC and Percent Difference (%) between Baseline (unit value) and Testing Data

Temperature. (°F)	Baseline 1: T=55°			Percent Difference (%)		
	M_1	M_2	M_3	M_1	M_2	M_3
4	0.9836	0.8631	0.9465	1.64	13.7	5.35
4	0.9891	0.9660	0.9502	1.09	3.4	4.98
10	0.9944	0.9513	0.9621	0.56	4.87	3.79
15	0.9858	0.9738	0.9373	1.42	2.62	6.27
18*	0.9881	0.0101	0.9407	1.19	98.99	5.93
18	0.9905	0.9930	0.9296	0.95	0.7	7.04
19*	0.9895	0.4685	0.9621	1.05	53.15	3.79
19*	0.9895	0.6191	0.9694	1.05	38.09	3.06
28	0.9785	0.9381	0.9084	2.15	6.19	9.16
29	0.9875	0.9974	0.9362	1.25	0.26	6.38
30	0.9893	0.9640	0.9804	1.07	3.6	1.96
37	0.9964	0.9890	0.8744	0.36	1.1	12.56
40*	0.9946	0.6304	0.7589	0.54	36.96	24.11
43	0.9959	0.9924	0.9694	0.41	0.76	3.06

* Bad data sets at the first torsional modal displacements

Table A3. (Continued)

Temperature. (°F)	Baseline 2: T=55°			Percent Difference (%)		
	M_1	M_2	M_3	M_1	M_2	M_3
4	0.9939	0.8001	0.9853	0.61	19.99	1.47
4	0.9972	0.9226	0.9861	0.28	7.74	1.39
10	0.9961	0.9187	0.9840	0.39	8.13	1.6
15	0.9953	0.9187	0.9939	0.47	8.13	0.61
18*	0.9971	0.0132	0.9931	0.29	98.68	0.69
18	0.9981	0.9548	0.9967	0.19	4.52	0.33
19*	0.9947	0.5221	0.9803	0.53	47.79	1.97
19*	0.9947	0.6000	0.9770	0.53	40	2.3
28	0.9843	0.8920	0.9495	1.57	10.8	5.05
29	0.9979	0.9677	0.8596	0.21	3.23	14.04
30	0.9985	0.8987	0.9738	0.15	10.13	2.62
37	0.9959	0.9424	0.9903	0.41	5.76	0.97
40*	0.9946	0.6441	0.6346	100	100	100
43	0.9959	0.9424	0.9903	0.41	5.76	0.97

Table A4. COMAC - Baseline 1

Temperature (°F)	Accelerometer No.					
	1	2	7	9	13	15
4	0.9295	0.9995	0.8242	0.8714	0.9383	0.9939
4	0.9655	0.9972	0.8616	0.9875	0.9648	0.9905
10	0.9914	0.9983	0.9966	0.9045	0.9717	0.9977
15	0.9411	0.9967	0.9889	0.9845	0.9438	0.9713
18	0.9617	0.9877	0.9891	0.9865	0.9763	0.9929
18*	0.4761	0.5586	0.9980	0.9879	0.5617	0.7164
19*	0.9834	0.5627	0.9792	0.9871	0.9806	0.9788
19*	0.9795	0.5623	0.9942	0.9875	0.9699	0.9749
28	0.9888	0.9756	0.9939	0.9849	0.9194	0.9555
29	0.9841	0.9848	0.9942	0.9310	0.9969	0.9858
30	0.9417	0.9940	0.9941	0.9871	0.9620	0.9941
37	0.9459	0.9548	0.9918	0.9861	0.9459	0.9937
40*	0.9795	0.5604	0.4788	0.9875	0.9793	0.9867
43	0.9776	0.9912	0.9965	0.9979	0.9981	0.9980

Table A4. (Continued)

Temperature (°F)	Accelerometer No.							
	3	4	6	8	10	12	14	16
4	0.998	0.99915	0.9939	0.86167	0.98423	0.95905	0.97897	0.96281
10	0.99695	0.88328	0.99998	0.98743	0.97957	0.9602	0.99777	0.98413
15	0.99437	0.998	0.98861	0.9289	0.98106	0.93957	0.97146	0.97023
18	0.99589	0.99973	0.97496	0.98914	0.95736	0.95005	0.99912	0.97143
18*	0.7273	0.99969	0.6228	0.3868	0.52183	0.58074	0.3323	0.57538
19*	0.99003	0.99955	0.6203	0.39362	0.93265	0.97325	0.8828	0.56348
19*	0.98677	0.99999	0.6184	0.39384	0.94574	0.9806	0.88009	0.9255
28	0.98273	0.94886	0.98299	0.99584	0.97799	0.95177	0.93484	0.99924
29	0.99967	0.97329	0.97705	0.95745	0.99734	0.99556	0.96437	0.99309
30	0.99253	0.99947	0.98611	0.94919	0.96769	0.934	0.9881	0.9854
37	0.97755	0.99981	0.9585	0.91519	0.95583	0.93962	0.98267	0.94907
40*	0.99511	0.48885	0.61416	0.20438	0.99309	0.96631	0.87986	0.98999
43	0.99501	0.99973	0.98431	0.99715	0.99541	0.98655	0.88707	0.99342

Table A5. Percent Difference of COMAC - Baseline 1

Temperature (°F)	Accelerometer No.					
	1	2	7	9	13	15
4	7.05	0.05	17.58	12.86	6.17	0.61
4	3.45	0.28	13.84	1.25	3.52	0.95
10	0.86	0.17	0.34	9.55	2.83	0.23
15	5.89	0.33	1.11	1.55	5.62	2.87
18	3.83	1.23	1.09	1.35	2.37	0.71
18*	52.39	44.14	0.2	1.21	43.83	28.36
19*	1.66	43.73	2.08	1.29	1.94	2.12
19*	2.05	43.77	0.58	1.25	3.01	2.51
28	1.12	2.44	0.61	1.51	8.06	4.45
29	1.59	1.52	0.58	6.9	0.31	1.42
30	5.83	0.6	0.59	1.29	3.8	0.59
37	5.41	4.52	0.82	1.39	5.41	0.63
40*	2.05	43.96	52.12	1.25	2.07	1.33
43	2.24	0.88	0.35	0.21	0.19	0.20

Table A5. (Continued)

Temperature (°F)	Accelerometer No.							
	3	4	6	8	10	12	14	16
4	0.2	0.085	0.61	13.833	1.577	4.095	2.103	3.719
10	0.305	11.672	0.002	1.257	2.043	3.98	0.223	1.587
15	0.563	0.2	1.139	7.11	1.894	6.043	2.854	2.977
18*	27.28	0.04	37.72	61.32	47.82	41.93	66.77	42.47
18	0.411	0.027	2.504	1.086	4.264	4.995	0.088	2.857
19*	1.323	0.001	38.16	60.616	5.426	1.94	11.991	7.45
28	1.727	5.114	1.701	0.416	2.201	4.823	6.516	0.076
29	0.033	2.671	2.295	4.255	0.266	0.444	3.563	0.691
30	0.747	0.053	1.389	5.081	3.231	6.6	1.19	1.46
37	2.245	0.019	4.15	8.481	4.417	6.038	1.733	5.093
40*	0.489	51.115	38.584	79.562	0.691	3.369	12.014	1.001
43	0.499	0.027	1.57	0.285	0.459	1.345	11.29	0.658

Table A6. COMAC - Baseline 2

Temperature (°F)	Accelerometer No.					
	1	2	7	9	13	15
4	0.9742	0.9875	0.8635	0.9991	0.9941	0.9943
4	0.9419	0.9800	0.8262	0.7901	0.9760	0.9963
10	0.9913	0.9886	0.9984	0.8298	0.9981	0.9992
15	0.9615	0.9950	0.9999	0.9997	0.9863	0.9738
18	0.9785	0.9935	0.9999	0.9999	0.9969	0.9937
18*	0.5164	0.5288	0.9970	0.9983	0.6480	0.7193
19*	0.9674	0.5160	0.9995	0.9976	0.9435	0.9751
19*	0.9889	0.5139	0.9978	0.9997	0.9981	0.9790
28	0.9901	0.9853	0.9995	0.9998	0.9752	0.9626
29	0.9689	0.9386	0.9697	0.9195	0.9821	0.9881
30	0.9488	0.9891	0.9995	0.9996	0.9865	0.9933
37	0.9704	0.9882	0.9999	0.9939	0.9896	0.9957
40*	0.9897	0.4989	0.3814	0.9987	0.9717	0.9859
43	0.9787	0.9904	0.9989	0.9980	0.9979	0.9988

* Bad data due to accelerometer temporary failure

Table A7. Comparisons of Modal Flexibility Using Data Processing Approach

Case No.	Not Using Data Processing Approach			Using Data Processing Approach		
	F1	F2	F3	F1	F2	F3
1	0.705	0.373	0.285	0.0771	0.0588	0.0362
2	0.662	0.356	0.249	0.0754	0.0577	0.0353
	Percent Difference (%) of case 1 & 2			Percent Difference (%) of case 1 & 2		
	6.01	4.36	12.43	2.19	1.909	2.603
1	0.705	0.373	0.285	0.0771	0.0588	0.0362
3	0.558	0.246	0.221	0.0615	0.0458	0.0300
	Percent Difference (%) of case 1 & 3			Percent Difference (%) of case 1 & 3		
	20.8	34.07	22.3	20.2	22.1	17.1

Table A8. Modal Flexibility and Percent Difference (%)

Temperature (°F)	Modal Flexibility (baseline 1)			Percent Difference (%)		
	F_1	F_2	F_3	F_1	F_2	F_3
4	0.06219	0.04488	0.02983	-19.4012	-24.1764	-16.5127
4	0.06127	0.04358	0.02993	-20.5935	-26.3726	-16.2328
10	0.06157	0.04605	0.02962	-20.2048	-22.1997	-17.1005
15	0.06409	0.04585	0.02952	-16.9388	-22.5376	-17.3804
18	0.06474	0.04565	0.03110	-16.0964	-22.8755	-12.9583
18*	0.06474	0.04585	0.03067	-16.0964	-22.5375	-14.1617
19*	0.06409	0.04520	0.03000	-16.9388	-23.6357	-16.0369
19*	0.06817	0.04767	0.03177	-11.6511	-19.4627	-11.0831
28	0.06677	0.04767	0.03223	-13.4655	-19.4627	-9.79569
29	0.07122	0.05070	0.03013	-7.69829	-14.3436	-15.6731
30	0.07506	0.05750	0.03480	-2.72162	-2.85521	-2.60285
37	0.07589	0.05862	0.03463	-1.64593	-0.963	-3.07865
40*	0.07305	0.05458	0.03202	-5.32659	-7.78848	-10.3834
43	0.07506	0.05862	0.03493	-2.72162	-0.963	-2.23901
Baseline	0.07716	0.05919	0.03573			

Table A8. (Continued)

Temperature (°F)	Modal Flexibility (baseline 2)			Percent Difference (%)		
	F_1	F_2	F_3	F_1	F_2	F_3
4	0.06218	0.04488	0.02983	-19.4142	-24.1764	-16.5127
4	0.06126	0.04358	0.02993	-20.6065	-26.3726	-16.2328
10	0.06157	0.04605	0.02962	-20.2048	-22.1997	-17.1005
15	0.06409	0.04585	0.02952	-16.9388	-22.5376	-17.3804
18	0.06474	0.04565	0.03110	-16.0964	-22.8755	-12.9583
18*	0.06474	0.04585	0.03067	-16.0964	-22.5375	-14.1617
19*	0.06817	0.04760	0.03177	-11.6511	-19.581	-11.0831
19*	0.06409	0.04526	0.03000	-16.9388	-23.5343	-16.0369
28	0.06676	0.04767	0.03223	-13.4785	-19.4627	-9.79569
29	0.07122	0.05072	0.03013	-7.69829	-14.3098	-15.6731
30	0.07506	0.05750	0.03480	-2.72162	-2.85521	-2.60285
37	0.07589	0.05862	0.03573	-1.64593	-0.963	0
40*	0.07035	0.05459	0.03202	-8.82582	-7.77158	-10.3834
43	0.07506	0.05860	0.03493	-2.72162	-0.99679	-2.23901
Baseline	0.07716	0.05919	0.03573			